DISSERTATION

ADVECTIVE-DIFFUSIVE GASEOUS TRANSPORT IN POROUS MEDIA: THE MOLECULAR DIFFUSION REGIME

Submitted by

John Merritt Farr

Department of Agricultural and

Chemical Engineering

In partial fulfillment of the requirements

for the Doctor of Philosophy Degree

Colorado State University

Fort Collins, Colorado

Spring 1993

COLORADO STATE UNIVERSITY

March 29, 1993

WE HEREBY RECOMMEND THAT THE DISSERTATION PREPARED UNDER OUR SUPERVISION BY JOHN M. FARR, ENTITLED ADVECTIVE-DIFFUSIVE GASEOUS TRANSPORT IN POROUS MEDIA: THE MOLECULAR DIFFUSION REGIME, BE ACCEPTED AS FULFILLING IN PART REQUIREMENTS FOR THE DOCTOR OF PHILOSOPHY DEGREE.

Committee on Graduate Work

Adviser

Department Head

ABSTRACT OF DISSERTATION

ADVECTIVE-DIFFUSIVE GASEOUS TRANSPORT IN POROUS MEDIA: THE MOLECULAR DIFFUSION REGIME

Traditional mathematical models for advective-diffusive transport in porous media fail to represent important physical processes when fluid density depends on composition. Such is the case for gas mixtures comprised of species with differing molecular masses, such as found in the vadose zone near chlorinated hydrocarbon sources.

To address problems of this nature, a more general advection-diffusion (A-D) model is presented, which is valid for porous media with permeabilities exceeding 10^{-10} cm^2 (where Klinkenberg and Knudsen effects are negligible). The new mathematical model is derived by thermodynamic means, based on identifying the meaning of Darcy's advective reference velocity in terms of a weighted average of species drift velocities. The resulting model has no additional parameters, and introduces no additional complexity or non-linearity when compared to the traditional A-D model most commonly used in hydrology and environmental science. Because the form of traditional A-D models is retained, the new formulations fit readily into existing numerical

simulators for the solution of subsurface transport problems.

The new model is equivalent to the Dusty-Gas Model of Mason *et al.* (1967) for cases where the molecular diffusion regime prevails and pressure, temperature, and forced diffusion are negligible. Further support of the model is provided by hydrodynamic analysis, accounting for the diffusive-slip flux identified by Kramers and Kistemaker (1943). The new model is analytically compared to two existing A-D models, one from the hydrology literature, where Darcy's law is assumed to yield a mass-average velocity, and one from the chemical engineering literature, where Darcy's law is assumed to yield a mole-average velocity. Significant differences are shown to exist between the three transport models. The new model is shown to match closely with the experimental data of Evans *et al.* (1961a), while the existing A-D models are shown to fail in this regard.

John Merritt Farr
Department of Agricultural and
Chemical Engineering
Colorado State University
Fort Collins, CO 80523
Spring 1993

ACKNOWLEDGMENTS

The author wishes to thank Professors Arnold Klute and David B. McWhorter for their help fostering the author's interest in critically examining the governing equations used in subsurface transport modeling. Additional thanks are extended to David McWhorter for his thorough review of manuscripts, and his valuable suggestions for improvements to the draft dissertation. Thanks are also due to the author's doctoral committee members, Edwin P. Weeks and Professors Daniel K. Sunada and Terry G. Lenz, for their guidance and assistance.

Funding for this research was provided by two sources: the Water Resources Division of the U. S. Geological Survey, and the University of Waterloo Solvents-in-Groundwater Research Program supported by contributions from Ciba Geigy, Dow Chemical, General Electric, and Eastman Kodak.

TABLE OF CONTENTS

LIST OF TABLES

LIST OF FIGURES

CHAPTER 1

INTRODUCTION

Background

This dissertation addresses the topic of gaseous transport in porous media. Existing deterministic mathematical models for simulating gaseous transport processes in porous media are critically examined, and an improved mathematical model for practical application is presented. Understanding gaseous transport in porous media is central to a wide array of applications, including the modeling of 1) chemical fate and transport in the environment, 2) the performance of vapor-dominated geothermal reservoirs, 3) drying processes for porous media, 4) reaction rates in porous catalysts, and 5) the performance of isotope separation processes and nuclear reactors.

The primary focus of this dissertation is the first application listed above: environmental transport modeling. Discussions focus on subsurface transport processes, although it is realized that subsurface processes can affect, or be affected by the surface and atmospheric environments through inter-compartmental fluxes. Discussion of transport within the non-gaseous phases of the subsurface is also neglected here, even though it is recognized that

gaseous transport cannot be understood or modeled effectively without consideration of all existing phases.

Over the past decade, several distributed parameter, multiphase, multicomponent numerical transport simulators (computer codes) have been developed for use in detailed analysis of subsurface transport processes. At the heart of each numerical simulator lies a governing mathematical model, derived from physical principles. The governing mathematical models for subsurface transport simulators used in environmental science and hydrology are of the advective-dispersive (A-D) form (i.e., the species fluxes are split into an advective term and a dispersive term). Analysis of particle Peclet numbers shows that mechanical dispersion is negligible compared to diffusion in porous media gas transport; thus, the "dispersive" term is a diffusion term, and "A-D" will refer to advection-diffusion in the remainder of this dissertation.

Due to the complexities of the processes involved, all of the models have been derived on the basis of simplifying assumptions. Although the recognized simplifying assumptions vary somewhat between models, the generality of existing A-D numerical transport simulators is limited due to implicit assumptions about the meaning of advective reference velocities that are invalid in certain cases of practical interest. It will be shown here that the common assumptions about the meaning of the Darcy advective velocity for fluid mixtures are invalid in cases where the

fluid (or phase) mass density depends significantly on phase composition (i.e., species concentrations).

The reliance on flawed assumptions about the Darcy advective velocity (described in detail later) has resulted in A-D models that combine inappropriate diffusion equations with Darcy's law, and these models do not properly handle cases where phase densities depend significantly on phase composition. When phase densities are highly dependent on composition, diffusive fluxes simulated by the commonly employed models can be significantly inaccurate, causing errors in transport predictions. Chemical transport in porous media is often significantly affected by, or dominated by diffusive fluxes, making the potential for modeling inaccuracies of concern in such cases. Gas-phase transport holds a greater potential for modeling inaccuracies than liquid-phase transport because diffusion coefficients for gases are much higher than for liquids, and because gas-phase densities can depend more strongly on composition. Such factors are important to consider when modeling gaseous transport of volatile organic compounds (VOCs) in the subsurface, a problem of great interest in environmental science and hydrology.

In A-D models, diffusive fluxes are referenced to advective velocities. The modeling framework of the classic transport phenomena literature (e.g., Bird *et al.*, 1960) provides the basis to derive flux equations for binary species diffusion relative to any advective reference

velocity that can be defined as a weighted average of species drift velocities. In the modeling of flow and transport in porous media, Darcy's law has been universally applied to describe the bulk flow component of transport and to serve as the advective reference velocity for diffusive fluxes. Despite the heavy reliance modelers have placed on Darcy's law, a critical examination of the Darcy reference velocity apparently has not been conducted. Specifically, it is important to understand what the Darcy velocity is comprised of, in terms of the species drift velocities in a mixture, when modeling transport in fluid mixtures having compositional density dependence.

A-D transport models used in the hydrologic community are based on the assumption that Darcy's law and Poiseuille's law yield a macroscopic mass-average velocity. In contrast, many chemical engineering models are based on the assumption that these same constitutive relations yield a mole-average velocity. These different assumptions result in two different A-D models that give different predictions for binary counter-diffusion fluxes in porous media or capillary tubes. Under isobaric conditions, the hydrologic models predict equimass fluxes and the chemical engineering models predict equimolar fluxes (Farr and McWhorter, 1988). As will be shown, neither of these model predictions match the reproducible experimental results of numerous researchers, which until very recently have gone unnoticed by the hydrologic community and much of the chemical

engineering community. Thus, there is a need for improved mathematical descriptions underlying the common transport models used in environmental problem solving.

The chemical physics and chemical engineering literature contain noteworthy derivations of complex mathematical models for the rigorous treatment of gaseous transport in porous media. Some of these models are capable of predicting the experimentally observed transport behavior mentioned above. They adequately represent transport in gases with compositional phase-density dependence, and some of these models represent multicomponent transport processes under more extreme gradients of pressure and temperature than are found under most environmental conditions. However, none of these models are couched in the form of traditional A-D models, and rigorous, distributed parameter numerical simulators have yet to be developed for these more complex mathematical models (which are generally implicit in the fluxes). Thus, there remains a need for a relatively simple model in the traditional A-D form that adequately represents gaseous transport in porous media for solving environmental problems of common interest. To properly derive an A-D model using the transport phenomena modeling framework requires detailed knowledge about the advective velocity given by Darcy's law. This dissertation addresses this critical requirement and provides an alternative formulation of the traditional A-D model for gaseous

transport in porous media in which the molecular diffusion regime prevails.

In porous media with pores that are large compared to the mean free paths of gaseous molecules contained within them, the molecular diffusion regime prevails, and diffusion is dominated by molecule-to-molecule collisions (rather than molecule-to-wall collisions). Under typical subsurface environmental pressures and temperatures, the molecular diffusion regime prevails in media with permeabilities above approximately 10^{-10} cm^2 (Evans *et al.*, 1961a; Klinkenberg, 1941; Massmann and Farrier, 1992). The new mathematical formulations presented here are valid only for porous media in which the molecular diffusion regime prevails. However, transport processes and applicable transport models for low-permeability porous media are briefly discussed.

Objectives

The broad objectives of this dissertation are to improve the level of understanding of transport processes in porous media and provide useful modeling tools for analyzing such problems. The dissertation deals primarily with gaseous transport, although the work has some implications for liquid-phase transport as well. The summary of historical literature on gaseous transport in porous media will serve to orient the reader as to the relevance, significance, and limitations of the modeling formulations derived here.

While retaining the simplicity and form of traditional A-D models, the modeling formulations presented here are more general and theoretically rigorous than A-D models currently in use. In addition, the new A-D model agrees more closely with experimental data, so improved accuracy in modeling predictions is expected. Because the new formulations retain the traditional A-D model form, they can be readily fitted into existing numerical modeling codes for solving engineering problems of practical interest.

Approach

Chapter 2 begins with conceptual process descriptions to illustrate the process complexities involved and the requirements for suitable mathematical models. The review of relevant historical literature provides the reader with an appropriate background to understand and appreciate the contributions of the dissertation.

In Chapter 3, new diffusion equations and a new A-D model for binary gaseous transport of mass and momentum in porous media are derived and discussed. Fundamental to the transport model is a new interpretation of the Darcy advective reference velocity in terms of species drift velocities. Support for the new model is provided by hydrodynamic analysis and by comparison to a limiting form of the more general (and complex) Dusty-Gas Model of Mason *et al.* (1967).

In Chapter 4, the transport model is compared to existing models and experimental data. The comparisons involve steady-state cases, for which analytical solutions are derived. The environmental conditions under which the new transport model is required (in order to obtain accurate results) are also discussed.

Chapter 5 presents a detailed comparison of the new transport model against the interdiffusion data of Evans *et al.* (1961a), showing that the model closely matches the experimental data. It is also shown that the existing A-D transport models fail to adequately represent the transport processes active during the experiments of Evans *et al.* Chapter 6 presents the conclusions of this dissertation.

CHAPTER 2

PROCESS DESCRIPTIONS AND LITERATURE REVIEW

This chapter contains conceptual process descriptions of gaseous transport in porous media, which are based on phenomenological interpretations of experimentally observed process behaviors. The discussion also serves to further define the modeling problem addressed here as a background for the literature review of existing models used to simulate the observed process behaviors. Much of the following discussion is based on the works of Cunningham and Williams (1980) and Mason and Malinauskas (1983).

Conceptual Process Descriptions

Although this dissertation focuses on processes occurring within the gas phase, it is recognized that important processes affecting gaseous transport in porous media occur outside the gas phase. Although generally less important for gases than vapors, species sorption, phase transfer, and transport in non-gaseous phases can significantly affect gas-phase transport. These effects, which can only be accurately represented in a multiphase transport model, will be treated in this dissertation only as they affect boundary conditions of the gas-phase. Thus,

the gas-phase models described here are meant to be incorporated into multiphase models for general transport simulations.

The observable transport of gases and their constituent species in porous media can be divided into four independent modes or mechanisms:

(1) Molecular diffusion, the process in which differing species in a gas mixture move relative to each other and relative to the bulk average movement of the mixture due to forces created by gradients in species concentration, pressure, and temperature, and due to external forces that act unequally on the different species. Molecular diffusion is controlled by molecule-to-molecule collisions, which dominate in cases where the flow domain (e.g., a pore channel) is large compared to the mean free path of gas molecules.

(2) Free-molecule or Knudsen transport, the process in which the movement of a given species is controlled only by its own concentration gradient. Knudsen transport is controlled by gas molecule-to-wall collisions, which dominate in cases with low gas density and/or very small pore sizes.

(3) Viscous flow, the process in which a bulk motion of the gas is driven by pressure gradients and gravitational forces. Viscous flow is controlled principally by molecule-to-molecule collisions, except near flow domain boundaries

(walls), where momentum transfer occurs by molecule-to-wall collisions.

(4) Surface diffusion, the process in which molecules move along the flow domain boundary in an adsorbed layer, driven by concentration gradients. Although surface diffusion can be important under certain conditions, it will not be discussed further in this dissertation. (An excellent discussion of surface diffusion is given by Carman (1956).)

In the general case, transport mechanisms (1) through (3) may act simultaneously, although one or two of these mechanisms usually dominate transport behavior. This dissertation deals primarily with the case where molecular diffusion is the dominant mechanism controlling transport behavior. Transport mechanisms (1) through (3) are discussed further, following a general discussion of the spatial scales used in conceptual and mathematical modeling. The discussions of viscous flow in this dissertation focus primarily on the viscous flow driven by pressure gradients.

Spatial Scales

Physical processes can be examined or modeled at various spatial scales, including the molecular, microscopic, macroscopic, and field scales. However, most of our experimental measurement devices and certainly our senses are restricted to the macroscopic and field scales. Thus, for practical applications, process description models

should be designed to operate at the macroscopic or field scales, using practically obtainable input data.

Our knowledge of small scale processes supports our knowledge of larger scale processes. Similarly, the larger scale models of continuum mechanics are based on the well-founded assumption that small scale process variables and physical properties can be averaged or integrated over larger volumes to yield predictable and more readily measurable larger-scale variables and physical properties. It is therefore instructive to begin our process descriptions at the molecular scale, even though practical models for transport modeling cannot be constructed at this scale.

Molecular-scale models describe the momenta, collisions, and resulting momentum transfers of individual molecules. The simple kinetic theory of gases views each molecule as a physical and mathematical point, occupying no volume. In contrast, microscopic and larger scale models are written in terms of the continuum variables of pressure, temperature, composition, and species drift velocities that must be defined over finite volumes of space. For the microscopic, macroscopic, and field scales, a distinction is made between physical (or material) "points" of finite volume and their corresponding mathematical points, which are located at the centroids of each physical point (Bear, 1972).

A generalized concept of representative elemental volumes (REVs - Bear, 1972) is useful in defining the microscopic, macroscopic, and field scales for continuum modeling problems. In terms of porous media transport, the microscopic REV is synonymous with a fluid "particle" or point, which is just large enough that the net effects of chaotic molecular-scale motions result in theoretically measurable pressures, temperatures, phase compositions, and fluxes that are locally stable under steady-state conditions. Typically, a microscopic REV resides completely within a single phase (e.g., within the pore gas). Due to current limitations in the size of sensors, the smoothly varying (continuous) fields of pressure, temperature, composition, and flux defined at the microscopic scale are practically impossible to measure within a porous medium.

The term "pore scale" is often used interchangeably with microscopic scale, although the size of a microscopic REV should be considered independent of pore size. Although microscopic REVs are much smaller than the pore diameters of most porous media, REVs for gases in porous media at low gas pressures or within small pores (e.g., in clays) can be larger than the pore diameters. In such cases, physical properties such as composition and pressure become discontinuous at the pore scale, and transport coefficients such as viscosity lose their continuum meanings. (This point will be elaborated on later.) As an example of the microscopic scale in a modeling application, the velocity

field given by Poiseuille's classic solution describes the radial distribution of microscopic-scale fluid velocity in a capillary tube.

While the molecular and microscopic scales lend themselves to relatively fixed REV definitions, the macroscopic scale definition can vary depending on the conceptual modeling approach and/or experimental measurement methods selected. The modeling approach and measurement methods selected should, in turn, be based on the type of problem to be solved. For example, the mathematical model describing total flow rate through a capillary tube (Poiseuille's law) is considered a macroscopic-scale model when compared to the microscopic-scale velocity distribution in the capillary. On the other hand, when the bundle of tubes analogy is used to derive (by volume averaging) a macroscopic-scale model such as Darcy's law for flow in porous media, Poiseuille's law could be viewed as a microscopic-scale model. To simplify things here, models such as Poiseuille's law, which result from the integration of microscopic-scale models, will be consistently referred to as macroscopic-scale models. The variables of fluid pressure, temperature, and flux as measured in laboratory columns of porous media are considered to be macroscopic-scale variables.

This dissertation does not explicitly address field-scale transport modeling, a task involving much in the way of empirical judgment. However, under certain field

conditions, the macroscopic-scale models presented in this dissertation can be applied directly to solve subsurface transport problems at the field scale with a reasonable level of confidence.

Processes

The movement or transport of an individual molecule is governed by momentum transfers resulting from collisions it has with "other" molecules. The other molecules may be of like or unlike species, with equal or unequal molecular mass. The other molecules can be suspended or dissolved in the same phase (e.g., the gas phase), or they can form part of the phase boundary, as in the walls containing a gas. During simple elastic molecular collisions, momentum and kinetic energy are conserved. The collisions and energy transfers between gas molecules are so frequent that, on the average, all of the molecules in a gas mixture have the same kinetic energy, dependent only on temperature. Because molecular kinetic energy is proportional to an individual molecule's mass, it follows that the average speed of lighter molecules exceeds that of heavier molecules. The pressure a gas exerts on a surface is the effect of molecular collisions with the surface. Fluid pressure is exerted in all directions, on neighboring walls and on the mathematical surfaces separating microscopic REVs. It is for this reason that the force due to a pressure gradient is termed a surface force. Because the magnitude of momentum

and kinetic energy transferred during each molecular collision is independent of molecular masses, pressure increases only as the molecular density and frequency of collisions increase.

System Without Walls

Assume for the moment that we are interested in analyzing transport in a volume of unconfined gas. This is the so-called "system without walls" described by Cunningham and Williams (1980). In such a system, wall effects such as viscous drag can be ignored. If the gas volume moves as a whole (i.e., bulk flow), the over-all velocity of the gas is superimposed on the temperature-dependent, random motion of individual molecules. It is convenient to view and analyze certain aspects of this system from a coordinate system moving with a velocity equal to the bulk advective gas velocity. The velocity of such a moving coordinate system will be referred to here as the advective reference velocity. To be useful for quantitative modeling purposes, the advective reference velocity must be defined mathematically. The advective reference velocity used in this section is defined as the net average velocity of the population of molecules contained within a microscopic REV, or the average molecular drift velocity. This advective reference velocity is termed a mole-average velocity, which can also be described as a mole-fraction weighted average of the species drift velocities in a mixture. (There are

several other ways to define an advective reference velocity, including the mass-average velocity, which is a mass-fraction weighted average of the species drift velocities in a mixture.)

When molecules of a given species in a gas mixture move with a drift velocity differing from the advective reference velocity, they are commonly said to be "diffusing" at a "diffusion velocity" equal to the difference between the species drift velocity and the advective reference velocity (Appendix A). The "diffusion flux" is the product of the diffusion velocity and the species concentration or density (in units of molecules or moles per volume). The diffusion flux, as defined here, refers to a segregative or nonadvective flux. The advective species flux is given by the product of the advective reference velocity and the species concentration.

In an unconfined gas initially at uniform pressure, any molecular concentration gradients (i.e., pressure gradients) that might develop due to internal forces are dissipated instantaneously without loss of internal momentum. For a single-species gas (pure gas), the system could aptly be described as completely stagnant, and our advective reference velocity would be zero. If, however, the gas is composed of multiple molecular species, the species' populations are free to move relative to each other, and the system can no longer be thought of as completely stagnant. Each species can move with its own drift velocity, but the

vectorial sum of species diffusion fluxes as defined here must sum to zero.

Consider the case of an unconfined, isothermal binary gas mixture with gradients in species concentration, but with uniform total pressure (i.e., uniform molecular concentration). In the presence of species concentration gradients in the general case (where the species have different molecular masses), excess pressure will "begin" to develop in regions of the gas mixture towards which the lighter, faster molecules move. In this hypothetical system without walls, the incipient pressure gradient is dissipated before it actually develops by instantaneous bulk movement of the gas mixture. Although no diffusion-induced pressure gradients can be observed in a system without walls, diffusion-induced advection still occurs. This hypothetical system would be impossible to model due to lack of adequate boundary conditions, and it could be argued that such a system does not exist in nature. The system without walls is, nevertheless, useful as a limiting conceptualmodel, highlighting the fact that diffusion-induced pressure gradients are impossible to detect in very open, high permeability systems.

Systems With Walls

The presence of containment walls alters gaseous transport behavior because momentum can be transferred between the gas and the walls. If gas molecule-to-wall

collisions resulted in specular reflections, the walls would dissipate little momentum. However, due to adsorption-desorption effects and the extremely rough nature of walls at the molecular scale, it has been shown that gas molecule-to-wall collisions result in diffuse reflections, with a mean reflection angle normal to the wall (Cunningham and Williams, 1980). If the bulk gas is moving, a component of velocity (and momentum) exists parallel to the wall. The diffuse reflection or scattering of gas molecules that collide with molecules of the wall results in dissipation of the momentum parallel to the wall (in the immediate vicinity of the wall). On a molecular scale, the gas molecules that are near the wall, but have not collided with it, end up colliding with wall-scattered molecules, and the momentum drag of the wall is translated away from the wall by these secondary collisions. On the microscopic scale, this translation and dissipation of momentum is described by Newton's law of viscosity.

Diffusion-Induced Pressure Gradients

Because momentum is transferred between the gas and the surrounding walls, sensible pressure gradients can develop in porous media gases where species with differing molecular mass are interdiffusing. When diffusion-induced pressure gradients go unnoticed during diffusion experiments, or they are ignored in conceptual modeling, significant misinterpretations and misunderstandings can result.

Most published diffusion coefficients are relatively accurate, perhaps somewhat fortuitously, because they were derived from flux measurements in closed systems where, by continuity, equimolar countercurrent transport must occur. In such cases, the common (but oversimplified) diffusion model, using a basic diffusion equation (equation (3-6)) and the unjustified assumption of no advective flux, yields correct diffusion coefficients. However, diffusion coefficients are also measured in open systems, as shown in Figure 4-1 and discussed in Chapter 5. The incorrect assumption that equimolar countercurrent transport in closed systems occurs isobarically leads to the use of the same simple model (e.g., diffusion equation (3-6)) to determine diffusion coefficients from both closed and (isobaric) open systems. If all species fluxes are measured during open-system experiments, the data readily show that equimolar countercurrent transport does not occur under isobaric conditions (see the experimental data in Chapter 5). On the other hand, if the flux of only one species is measured, and the molar flux of the other species (in a binary gas) is assumed equal and opposite, erroneous diffusion coefficients will result for gas mixtures with species of differing molecular mass. These are important considerations when designing experiments and conducting analyses to determine diffusion coefficients from experimental data.

The nature and relative importance of wall effects depends on the distance between the flow domain walls (e.g.,

pore diameter), and the average distance between molecular collisions, or the "mean free path". When the pore diameters are large compared to the mean free path of the gas molecules, diffusive and viscous transport can be modeled at the pore scale as continuum processes (using microscopic REVs), and macroscopic models can be derived by integrating pore-scale model equations over macroscopic REVs. This scaling integration results in the creation of terms accounting for the macroscopic transport effects of porous media porosity and tortuosity.

In the limiting case of Knudsen transport, where the mean free path is very large compared to pore diameters, only gas molecule-to-wall collisions occur. In this case, the movement of each molecule is controlled separately by the wall effects (i.e., there is no momentum transfer between gas molecules), and the concept of viscosity used in continuum models for larger-pore media is meaningless. There is no viscous flow in this limiting case, and the transport model used for the Knudsen regime contains only terms describing species fluxes due to species concentration gradients. Another distinction is that the microscopic REV of the Knudsen transport model contains numerous pore channels and porous media solids. Thus, for practical purposes, microscopic and macroscopic models for Knudsen transport are equivalent and contain no porosity or tortuosity factors.

Knudsen transport accounts for the Klinkenberg effect (Klinkenberg, 1941); in fact, these two terms apply to the same phenomenon. The Klinkenberg effect is thought of as a phenomenon associated with pure gases, where as the term Knudsen transport is most commonly used to refer to species transport in gas mixtures. In any case, the mathematical model derived in Chapter 3 applies to systems with walls, where the pore sizes are large compared to the mean free path of gas molecules. In such cases, Knudsen (and Klinkenberg) effects can be neglected.

Until recently, the hydrologic literature and much of the chemical engineering literature (including major chemical engineering textbooks) overlooked the phenomena responsible for diffusion-induced pressure gradients. One of the traditional assumptions in chemical engineering has been that *equimolar* countercurrent diffusion occurs under isobaric conditions (Bird *et al*, 1960; Fahien, 1983; Cussler, 1984). Although this assumption is not stated explicitly in the references just cited, the relevant A-D transport models used by these authors reflect this assumption. In the hydrologic literature, no explicit assumption seems to have been made, although the common hydrologic A-D transport models predict *equimass* horizontal countercurrent diffusion under isobaric conditions (e.g., Whitaker, 1977; Hassanizadeh and Gray, 1979a,b; Abriola and Pinder, 1985; Pollock, 1986; Kipp, 1987; Pruess, 1987; Falta *et al.*, 1989, 1992). The A-D models from both chemical

engineering and hydrology represent the advective flux using Darcy's law, which predicts no horizontal flux in an isobaric system.

It is shown mathematically in Chapter 3 that the difference between the existing A-D transport models is due to the fact that the chemical engineering model implicitly assumes that Darcy's law yields a mole-average advective reference velocity and the hydrology model implicitly assumes that Darcy's law yields a mass-average advective reference velocity. It is shown in Chapter 3 that neither of these assumptions is correct, and a new interpretation of the Darcy advective reference velocity is offered.

Thought Experiment

The following thought experiment is presented to show, at least conceptually, why Darcy's law does not yield a mass-average velocity. The thought experiment, along with further discussion that relies on experimental data, will also show why Darcy's law does not yield a mole-average velocity. Consider a case of binary countercurrent diffusion within an isothermal porous medium where Knudsen transport is negligible. Within a closed-ended horizontal column of moist sand, the two gaseous species of a binary mixture are initially distributed as shown in Figure 2-1. Species A is 1,1-dichloroethylene (1,1-DCE), with a molecular mass of M_A = 96.94 g/mole. Species B is moist air, with a mole-averaged molecular mass of M_B = 28.7 g/mole

for the mixture of N_2, O_2, and CO_2, saturated with water vapor at 20°C and 1 atmosphere pressure. The binary gas mixture in such a case would behave ideally.

Examine first the hypothetical case where pressure and temperature are held constant throughout the column (at 1 atm and 20°C) as the initial concentration gradients shown in Figure 2-1 dissipate due to countercurrent diffusion. The density of the moist air saturated with 1,1-DCE at the right-hand end of the column is 3.04 g/L, or 2.55 times the density of the pure moist air at the left end of the column. The initial center of mass in the gas phase lies off center, at x = 28.6 cm, toward the end of the column where the heavier species, 1,1-DCE, is concentrated.

The barycentric or mass-average advective velocity describes the motion of the center of mass in a fluid. In the gas mixture of our thought experiment, a mass-average velocity can be seen to exist when no Darcy flux is expected to occur. As the two species interdiffuse with time, the center of mass moves to the center of the column, and a finite mass-average velocity exists until the concentration gradients within the column vanish. The Darcy seepage velocity equals zero under horizontal, isobaric conditions, leading to the (as yet poorly supported) conclusion that the Darcy seepage velocity is not equivalent to a mass-average velocity for cases when the phase density varies with composition.

The fact that Darcy's law does not yield a mass-average velocity is not actually proven by this somewhat misleading thought experiment, which also leads to the erroneous conclusion that Darcy's law yields a mole-average velocity. Farr and McWhorter (1988) correctly made the former conclusion above, and incorrectly made the latter conclusion as well, based on this type of thought experiment. The flaw in the thought experiment is the incorrect assumption that pressure remains constant during countercurrent diffusion in a closed system.

As alluded to previously, a diffusion-induced pressure gradient develops in closed systems, and a viscous flux (described by Darcy's law) results. The common hydrologic transport model predicts equimass countercurrent diffusion under the initially isobaric conditions described in the thought experiment. In a binary gas comprised of species with differing molecular masses, the equimass countercurrent diffusion predicted by the hydrologic transport model is nonequimolar, resulting in the development of a pressure gradient. The hydrologic model thus predicts a diffusion-induced pressure gradient and an associated viscous flux for such a system, although theoretical and experimental evidence shows that the predicted magnitudes of the pressure gradient and viscous flux are too large. It is surprising that this model-predicted, diffusion-induced pressure gradient went unnoticed by the hydrologic community for so long.

The assumption of equimolar countercurrent diffusion in closed binary systems is founded on experimental flux data. Until recently, however, most researchers studying diffusion did not make pressure measurements during their experiments. Thus, the diffusion-induced pressure gradients that occur in closed systems went undetected (although as pointed out previously, diffusion-induced pressure gradients are extremely difficult to detect in highly permeable media).

The processes that lead to equimolar countercurrent diffusion in a closed system can be described as follows. Consider a closed-ended horizontal column of porous medium (as shown in Figure 2-1) where the gas phase is initially isobaric, and countercurrent diffusion of two components of differing molecular mass begins. At a given temperature, the molecules of both species have the same kinetic energy, and thus the lighter molecules must move with greater average speed than the heavier molecules. This results in a greater initial molar flux of the lighter component toward the end of the column where the heavier component is concentrated than vice versa, as indicated by the differing length of initial flux vectors on Figure 2-1. Pressure builds up at the end where the heavier component is initially more concentrated, and the diffusion-induced pressure gradient drives a non-segregative flux of the entire gas phase toward the end of the column where the lighter component is initially concentrated. In closed systems (such as those commonly used to measure diffusion

coefficients), this flux is exactly the right magnitude to balance out the fact that the initially isobaric countercurrent diffusion is not equimolar, but rather follows Graham's law, which states that the molar flux ratio equals the negative square-root of the inverse ratio of species molecular masses.

The advective-diffusive transport that occurs in closed systems, such as the Loschmidt-type diffusion cell, has been commonly observed and interpreted to be simply equimolar countercurrent diffusion in the absence of advection. In general, gaseous equimolar countercurrent diffusion occurs only in the presence of a pressure gradient.

Literature Review

This literature review discusses the relevant aspects of previous work that bear directly on the contents of this dissertation. Additional citations and discussions of relevant work are contained throughout the dissertation, where appropriate.

The primary contribution relied upon in this dissertation is that of Thomas Graham (1833), whose work is discussed in several more easily obtained references (Mason and Kronstadt, 1967; Mason and Evans, 1969; Cunningham and Williams, 1980; Cussler, 1976, 1984; Jackson, 1977; Mason and Malinauskas, 1983). The discussion below about Graham's work is based on the descriptions provided in these references.

Graham conducted gas diffusion experiments using a procedure he developed to ensure that isobaric conditions were maintained during the diffusion process. He used a simple diffusion tube consisting of a calibrated glass tube, plugged at one end with porous plaster about 1/5 inch thick. The open end of the tube was immersed in a vessel of water or mercury. The gas to be investigated was added to the tube by displacement of the liquid, and its standard volume was noted. During his initial experiments, Graham noted that as the subject gas diffused out of the tube and ambient air diffused in, the liquid level in the tube tended to rise or fall, depending on whether the gas was lighter or heavier than air, respectively. He noted that such changes in liquid level would produce pressure differences across the porous plug and make interpretations of the experimental results difficult. He therefore kept the pressure uniform by flowing water or mercury into or out of the outer vessel to keep the outer liquid level equal to that inside the tube.

Graham reported diffusion measurements for 10 gases, and concluded that molar isobaric gas diffusion was inversely proportional to the molecular mass of the gas. He further concluded that binary flux ratios during countercurrent gas diffusion could be described by what is now referred to as Graham's law of diffusion, equation (3-16). In his experiments using water (for gases with low aqueous solubility) Graham measured flux ratios to 5

significant figures, and his measurements compare favorably in accuracy to the best of recently published data. For the gases Graham tested with mercury, the reported flux ratios are, of course, less precise due to the increased difficulty in maintaining isobaric conditions with the denser liquid. It is noteworthy that the porous plaster used by Graham had large pores compared to the mean free path of gas molecules, and thus the molecular diffusion regime prevailed during his experiments.

Knudsen (1909) independently found that gases at low pressures or in very low permeability media interdiffuse according to the same law that Graham had discovered 76 years earlier, even though the transport mechanisms active in the Knudsen regime differ significantly from those active in the molecular diffusion regime. Although Knudsen's work came much later in time than Graham's, it was understood and accepted earlier than Graham's work.

Klinkenberg (1941) built on the ideas of Knudsen, and developed a practical method for determining the intrinsic permeability of a porous medium using multiple gas-flow measurements. Klinkenberg's method involves making several effective permeability measurements using a pure gas at several different pressures. The measured effective permeabilities are extrapolated to find the intrinsic permeability effective at high pressures, where Knudsen and Klinkenberg effects are negligible. The Klinkenberg effect is a direct result of Knudsen transport behavior, and the

onset of Klinkenberg effects at lower gas pressure or in lower permeability media marks the entry into the transition transport regime, which lies between the molecular diffusion regime and the Knudsen transport regime. Thorstenson and Pollock (1989) present a method for estimating effective Knudsen diffusion coefficients from the "Klinkenberg factor", as determined by the Klinkenberg method.

Numerous investigators have also shown that countercurrent diffusion flux ratios follow Graham's law of diffusion over the entire transition from the molecular regime to the Knudsen regime (Hoogschagen, 1953, 1955; Evans *et al.*, 1961a,b, 1962a,b, and 1963; Wicke and Hugo, 1961; Wakao and Smith, 1962; Rothfeld, 1963; Mason *et al.*, 1967; Satterfield and Cadle, 1968; Gunn and King, 1969; Remick and Geankoplis, 1973; and Alzaydi *et al.*, 1978). In addition to the references already cited, significant general contributions to the understanding of gaseous transport in capillaries and porous media have been made by Poiseuille (1846), Darcy (1856), Adzumi (1937a,b,c,d), Kramers and Kistemaker (1943), Carman (1956), Scott and Dullien (1962a,b), and Feng and Stewart (1973). For further discussion of the historical literature pertaining to gaseous transport in porous media, the reader is referred to Cunningham and Williams (1980).

A simple explanation for Graham's law of diffusion is based on the calculation of momentum transfer to the walls of the porous medium (e.g., the porous plaster plug of

Graham's experiments) by interdiffusing gases. This explanation was first presented by Hoogschagen (1955). The premise of the explanation is that no net force exists on the porous medium in the absence of a pressure gradient. The gases exert force on the porous medium only by gas molecule-to-wall collisions, and with no net force on the medium, the molecule-to-wall collisions must result in no net momentum transfer to the medium. This implies that the momentum transferred to the porous medium by one gas species must be counterbalanced by an equal, but oppositely directed transfer of momentum to the medium by the other species. The momentum transferred to the medium by a gas species per unit time equals the mean momentum transferred per molecular collision (which is proportional to the species molecular mass times its drift velocity, $M_i v_i$) multiplied by the number of molecular collisions per unit time (which is proportional to the species mean molecular speed times its molar concentration, $C_i c_i$). The sum of momenta transferred from the gas to the porous medium must equal zero under isobaric conditions. For a binary system,

$$(M_A \mathbf{v}_A)(C_A c_A) = (M_B \mathbf{v}_B)(C_B c_B) \tag{2-1}$$

or

$$\frac{C_A \mathbf{v}_A}{C_B \mathbf{v}_B} = \frac{M_B C_B}{M_A C_A} \tag{2-2}$$

The left-hand side of equation (2-2) defines the countercurrent molar flux ratio, and the mean molecular

speed, C_i, is inversely proportional to the square root of species molecular mass. Therefore, equation (2-2) is equivalent to Graham's law of diffusion, equation (3-16). Mason *et al.* (1967) show that Graham's law is easily extended to the multicomponent case shown in equation (3-24).

The mathematical physics of molecular diffusion has been studied for many years, with early contributions made by Maxwell (1860, 1867) and Stefan (1871, 1872). Based on momentum transfer arguments, they each independently derived the so-called Stefan-Maxwell Equation for multicomponent diffusion. The Stefan-Maxwell Equation provides an accurate description of isobaric, isothermal molecular diffusion, although it is implicit in the fluxes. Chapman and Cowling (1939) developed the rigorous molecular theory of gases, accounting for second order effects, such as pressure and thermal diffusion. Chapman and Cowling's work served as the basis for the subsequent developments of Pollard and Present (1948), Hirschfelder *et al.* (1954), Bird (1956), and deGroot and Mazur (1962).

The significant contribution of Kramers and Kistemaker (1943) is relied on directly to support the transport model developed in this dissertation. Based on the momentum transfer arguments first introduced by Maxwell, Kramers and Kistemaker showed that a diffusive-slip boundary condition on the mass-average velocity is required for proper solution of the Navier-Stokes Equation to describe the bulk motion of

gas mixtures with species of differing molecular mass. Kramers and Kistemaker also identified the "pressure effect" (or diffusion-induced pressure gradient) that occurs in closed systems during countercurrent gas diffusion. Although Kramers and Kistemaker did not present diffusion equations or a general transport model, per se, it appears that they used the key elements of the transport model developed in this dissertation. This aspect of Kramers and Kistemaker's work has not been recognized in the more recent literature, probably due to the disguised form of their equations and the fact that their presentation focused on the hydrodynamic effects of diffusive slip on bulk fluid motion. It was only after the equations presented in this dissertation were derived that this writer recognized their similarity to equations presented in Kramers and Kistemaker (1943). The new equations presented in this dissertation were derived in a different manner than Kramers and Kistemaker's, increasing the significance of the fact that both sets of equations are in agreement.

Finally, Evans *et al.* (1961b and 1962b) and Mason *et al.* (1967) made significant contributions with their development of the Dusty-Gas Model (DGM). The paper of Mason *et al.* (1967) presents the final (and corrected) version of the DGM; further discussion of the DGM is provided by Cunningham and Williams (1980) and Mason and Malinauskas (1983). This model has become the standard against which others are measured (Thorstenson and Pollock,

1989; Abriola *et al.*, 1992; and Massmann and Farrier, 1992). The DGM is derived using the rigorous molecular theory of gases, with the conceptual premise that the walls of the porous media solids can be represented as mega "molecules" constrained in space. The constitutive relations that resulted from the derivation of Mason *et al.* (1967) have been shown to accurately represent gaseous transport over the entire range from the Knudsen regime to the molecular diffusion regime. In its general form, however, the DGM includes a minimum of four parameters: permeability, tortuosity, porosity, and the Knudsen diffusivity of at least one of the gas species present. The DGM also has a complex form that is implicit in the fluxes, and for cases where the molecular diffusion regime prevails, the complexity of the DGM is not warranted.

The A-D gaseous transport model presented in Chapter 3 is offered as an alternative to the DGM for cases where the molecular diffusion regime prevails. This model is much easier to understand and use than the DGM, especially for workers already familiar with the modeling framework of the traditional transport phenomena literature (e.g., Bird *et al.*, 1960). As discussed in Chapter 5, the new model has only three parameters: permeability, tortuosity, and porosity. This makes the model easier to calibrate and use for predictive purposes than the DGM.

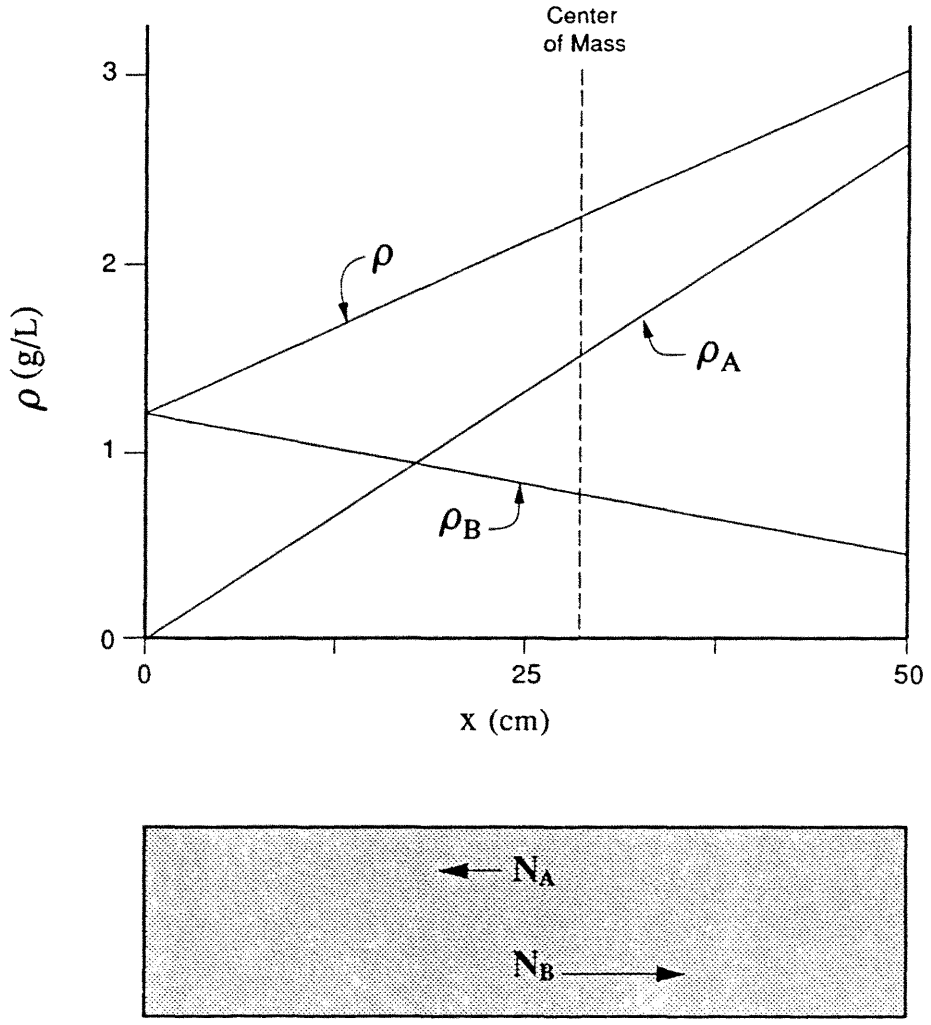

Figure 2-1. Assumed distributions and the "initial" molar fluxes of 1,1-DCE (A) and air (B) within a closed horizontal column of porous media at the start of countercurrent transport.

CHAPTER 3

MATHEMATICAL MODEL DEVELOPMENT

Background

In this chapter, governing equations for gaseous transport in porous media are derived, and theoretical support is provided for the resulting mathematical model. Further support for the new transport model is provided in Chapters 4 and 5 by comparisons to experimental data. The mathematical model consists of continuity equations incorporating constitutive equations for advective and nonadvective fluxes, plus state equations relating the system variables. To familiarize the reader with variables used in the following derivations, Appendix A contains a listing of equations relating various units of species concentration, drift velocities, and flux in binary systems.

As pointed out in Chapter 1, there are several reasons for enhancing the generality of traditional A-D models with improved diffusion equations. When modeling gaseous transport in porous media in which Klinkenberg and Knudsen effects are negligible, and when multicomponent diffusion effects are small, the complexities of the most general diffusion models, such as the Dusty Gas Model (DGM - Mason *et al.*, 1967) can be avoided. Traditional A-D models have

not been successfully applied to predict the Graham's law behavior described in Chapter 2 because of misunderstandings as to what the Darcy seepage velocity represents in terms of a weighted average of species drift velocities. From the observed transport behavior described by Graham's law, the form of the weighted average of species drift velocities (or the advective reference velocity) given by either Darcy's law or Poiseuille's law is derived here. This provides the basis to derive more general diffusive flux equations for cases where the molecular diffusion regime prevails. Equations for binary molecular diffusion flux relative to the newly identified advective reference velocity (the "Graham-average" velocity) are derived on both a molar and a mass basis. The resulting diffusion equations are then shown to be equivalent to the DGM, simplified for the molecular diffusion regime in the absence of forced, thermal, and pressure diffusion.

A modified Poiseuille's law, derived from molecular momentum transfer arguments justifying the use of a diffusive-slip boundary condition (Kramers and Kistemaker, 1943; Jackson, 1977) is also shown to directly yield the Graham-average advective velocity for flow in tubes. Using the "bundle-of-tubes" analogy, this modified Poiseuille's law lends further support to the new molecular diffusion equations for transport in porous media.

Finally, the new molecular diffusion equations are combined with appropriate continuity equations to complete

the mathematical formulation of a general A-D model for binary species transport of mass and momentum in porous media where forced, thermal, and pressure diffusion are considered negligible. As shown in subsequent chapters, the relatively simple A-D model presented here appears to adequately represent gaseous transport for most cases of environmental interest, including those with significant compositional dependence in the gas-phase density.

Derivation and Support of Constitutive Relations

Preliminaries

Let $\boldsymbol{v}_i$ represent the mean velocity of species i molecules within a representative elemental volume of gas mixture. This quantity is referred to here as the species drift velocity. The total molar flux of species i relative to stationary coordinates (i.e., fixed to the porous media) is then given by

$$\boldsymbol{N}_i = c_i \boldsymbol{v}_i \tag{3-1}$$

where c_i is the molar concentration of species i. This representation of total species flux is commonly separated into two terms representing advective and nonadvective fluxes, respectively. There are many different ways to separate the total species flux, resulting in different mathematical formulations. The nonadvective flux term is commonly referred to as the diffusive flux term, although many mathematical representations used for this term do not

correspond directly to the entire flux caused by diffusive processes.

A nonadvective flux can be defined relative to any convenient advective reference velocity. For example, the nonadvective molar flux relative to the mole-averaged advective velocity is defined by

$$\boldsymbol{J}_i^{NN} = c_i(\mathbf{v}_i - \mathbf{v}^N) \tag{3-2}$$

where the mole-average velocity is a weighted average of species drift velocities

$$\mathbf{v}^N = \frac{\Sigma c_i \mathbf{v}_i}{\Sigma c_i} = \frac{\Sigma c_i \mathbf{v}_i}{c} \tag{3-3}$$

and c is the total molar concentration of the mixture. A common alternative to equation (3-2) describes the nonadvective mass flux relative to the mass-averaged or barycentric advective velocity

$$\boldsymbol{J}_i^{MM} = \rho_i(\mathbf{v}_i - \mathbf{v}^M) \tag{3-4}$$

where the mass-average velocity is given by

$$\mathbf{v}^M = \frac{\Sigma \rho_i \mathbf{v}_i}{\Sigma \rho_i} = \frac{\Sigma \rho_i \mathbf{v}_i}{\rho} \tag{3-5}$$

and ρ is the total mass density of the mixture. Nonadvective fluxes can be defined with respect to other reference velocities, such as the volume-average velocity or the weight-equivalent average velocity (Bird *et al.*, 1960; Clazie, 1967; Cussler, 1984). A given problem should be analyzed using the most convenient nonadvective flux,

defined relative to an advective flux that is known a priori or given by a known constitutive relation.

Later in this chapter, a new advective reference velocity will be identified and a nonadvective flux will be defined relative to it. This new nonadvective flux will be shown to be most convenient for the analysis of gaseous transport in porous media because its advective reference velocity is that given by Darcy's law. The new nonadvective flux will also be shown to be a true "diffusive flux," accounting for the entire flux caused by diffusive processes in cases where the molecular diffusion regime prevails.

It is useful to write diffusive flux expressions in the form of a driving force (e.g., a concentration gradient) times a transport coefficient. Several different molecular diffusion equations of this form, including equations for $\mathbf{J}_i^{NN}$ and $\mathbf{J}_i^{MM}$ as defined in equations (3-2) and (3-4), have been derived based on kinetic theory and nonequilibrium thermodynamics (Hirschfelder *et al.*, 1954; Bird, 1956; Bird *et al.*, 1960; de Groot and Mazur, 1962). Both multicomponent and binary diffusion equations exist, although most of the discussion here is limited to the binary case, where the summations listed in equations (3-1) through (3-5) are taken from $i = A$ to $i = B$, and $D_{AB} = D_{BA}$. Excellent discussions of multicomponent diffusion are given by Bird *et al.* (1960), Clazie (1967), and Cussler (1976).

In general, diffusion can be driven by gradients in species mole fractions, pressure, and temperature. In

addition, variations in external forces acting on different species in a mixture can result in diffusive flux. Such "forced diffusion" can be significant in ionic systems, where the influence of electric fields tends to segregate charged species (Clazie, 1967). However, this dissertation does not deal with ionic systems, so forced diffusion will be neglected.

There is a unanimous literature consensus that temperature diffusion is not significant in environmental problems, or even in most chemical engineering applications (Hirschfelder *et al.*, 1954; Bird *et al.*, 1960; Cussler, 1984; Thorstenson and Pollock, 1989; Abriola *et al.*, 1992). Although more important than thermal diffusion, the general literature consensus indicates that pressure diffusion can also be reasonably neglected under typical environmental conditions (Bird *et al.*, 1960; Cussler, 1984).

Neglecting pressure diffusion is particularly justifiable in porous media in which the molecular diffusion regime prevails, and large gaseous pressure gradients are not expected to develop naturally (Thorstenson and Pollock, 1989). In such media, when pressure gradients are large enough to cause pressure diffusion to become an appreciable fraction of the total diffusive flux, diffusion (ordinary and pressure) is expected to be insignificant compared to the advective transport due to viscous flux. For gaseous transport in porous media in which the molecular diffusion regime prevails, ordinary molecular diffusion (driven by

gradients in species mole fraction) is expected to account for the vast majority of diffusive flux in cases of environmental interest. Thus, pressure, temperature, and forced diffusion fluxes will be neglected in the following derivations.

Note that although ordinary gaseous diffusion is shown in some references to be driven by gradients in species partial pressure (e.g., deGroot and Mazur, 1962; Cussler, 1976, 1984), the diffusion equations given by Bird (1956) and Bird *et al.* (1960), which show ordinary diffusion to be driven by gradients in species mole fraction, are taken to be more general and are used throughout this dissertation.

For the molecular diffusion regime, the molar diffusion flux of species *A* relative to the mole-average velocity in a binary mixture is given by (Bird *et al.*, 1960)

$$J_A^{NN} = -cD_{AB}^{*}\nabla\chi_A \qquad (3\text{-}6)$$

where D_{AB}^{*} is an effective binary diffusion coefficient, accounting for the porosity and tortuosity of a porous media, or simply equal to the free-space binary diffusion coefficient for diffusion in open tubes. The force gradient in equation (3-6) is expressed in terms of χ_A, the mole fraction of species *A* in the mixture. J_A^{NN} can also be expressed in terms of a gradient in mass fraction (Bird *et al.*, 1960)

$$J_A^{NN} = \frac{-\rho^2}{cM_AM_B} D_{AB}^* \nabla \omega_A \tag{3-7}$$

where M_A and M_B are the molecular masses of species A and B, respectively.

The mass flux of species A relative to the mass-average velocity of a binary mixture is given by (Bird *et al.*, 1960)

$$J_A^{MM} = -\rho D_{AB}^* \nabla \omega_A \tag{3-8}$$

or in terms of a gradient in mole fraction (Bird *et al.*, 1960)

$$J_A^{MM} = \frac{-c^2 M_A M_B}{\rho} D_{AB}^* \nabla \chi_A \tag{3-9}$$

Recognizing that $\rho = c(\chi_A M_A + \chi_B M_B)$ (Appendix A), equation (3-9) can be rewritten in terms of a molar flux of species A

$$J_A^{NM} = -\left[\frac{M_B}{M_A\chi_A + M_B\chi_B}\right] cD_{AB}^* \nabla \chi_A \tag{3-10}$$

Another common advective reference velocity is the volume-average velocity, favored by Cussler (1976, 1984)

$$\mathbf{v}^v = \sum \rho_i \frac{\overline{V}_i}{M_i} \mathbf{v}_i \tag{3-11}$$

where $\overline{V}_i$ is the partial molar volume of species i in the mixture. A volume-average velocity is equivalent to a mole-average velocity when the total molar concentration, c, is independent of phase composition. This is the case for ideal gases, where the partial molar volumes of the species equal the molar volume of the mixture. Such is the case for

gases and vapors under most environmental conditions, which are near atmospheric pressure and temperature.

The mass flux relative to a volume-average velocity is defined by

$$\mathbf{J}_i^{MV} = \rho_i(\mathbf{v}_i - \mathbf{v}^V) \tag{3-12}$$

In terms of a mass-fraction gradient, the mass flux of species *A* relative to a volume-average velocity in a binary mixture is given by

$$\mathbf{J}_A^{MV} = -\rho^2 \frac{\overline{V}_B}{M_B} D_{AB}^* \nabla\omega_A \tag{3-13}$$

where $\overline{V}_B$ is the partial molar volume of species *B*. Nearly equivalent to this expression is the mass flux relative to a mole-average velocity

$$\mathbf{J}_A^{MN} = \frac{-\rho^2}{CM_B} D_{AB}^* \nabla\omega_A \tag{3-14}$$

If the gas mixture behaves ideally, the partial volume of species *B* equals the molar volume of the mixture, $\overline{V}_B = V^o = 1/c$, and equations (3-13) and (3-14) are equivalent.

When using diffusion fluxes such as defined by equations (3-13) and (3-14), where the flux units do not correspond to the advective reference velocity, the sum of diffusive fluxes for all species in a phase will not equal zero. This is important when formulating a continuity equation for the fluid phase; the resulting transport model will have less terms if the species diffusion fluxes sum to zero for the phase mixture. Diffusion fluxes only sum to

zero when they are defined such that the flux units correspond to the advective reference velocity (e.g., mass flux relative to a mass-average velocity).

The diffusion equations given above are all quite general (completely general for ideal gases - Bird *et al.*, 1960), but they describe "diffusive" fluxes differently, as illustrated by the different definitions given by equations (3-2), (3-4), and (3-12). Lack of appreciation for the differences in the various diffusion equation forms can lead to their misuse and the misinterpretation of associated modeling results.

Another source of confusion surrounds the very common use of a less general binary diffusion equation given by

$$\boldsymbol{J}_A^{M?} = -D_{AB}^{*}\nabla\rho_A \qquad (3\text{-}15)$$

which describes mass flux relative to either a mass-average velocity (for constant mass density fluids) or a mole-average velocity (for constant molar density fluids). Despite the limitations of equation (3-15), it is commonly applied by modelers in hydrology and environmental science. Because we are concerned here with cases where the mass density can be a function of fluid composition (as well as pressure and temperature), equation (3-15) is presented here for reference purposes only. All of the binary diffusion equations given above can be written for the species *B* flux by simply exchanging the *A* and *B* subscripts.

As will be shown in Chapters 4 and 5, the various diffusion flux equations given above can yield significantly

different flux values under common conditions of environmental interest. Textbooks in chemical engineering recommend the use of equation (3-6) for modeling gaseous transport in tubes or packed columns of porous catalyst (e.g., Bird *et al.*, 1960; Fahien, 1983; Cussler, 1984). The use of equation (3-6) in a molar continuity equation with Poiseuille's law or Darcy's law to model chemical transport in tubes or porous media, respectively, relies on the implicit assumption that Poiseuille's law and Darcy's law yield macroscopic mole-averaged velocities.

In contrast, most subsurface transport models use equation (3-8) to describe diffusion fluxes, thereby taking the Darcy seepage velocity as a macroscopic mass-average velocity (e.g., Whitaker, 1977; Hassanizadeh and Gray, 1979a,b; Abriola and Pinder, 1985; Pollock, 1986; Kipp, 1987; Pruess, 1987; Falta *et al.*, 1989, 1991, 1992). Other subsurface transport models (e.g., Corapcioglu and Baehr, 1987; Jury *et al.*, 1983 and 1990, Sleep and Sykes, 1989; Mendoza and Frind, 1990) use the less general form of the diffusion flux given by equation (3-15).

For common chemical engineering applications, equation (3-6) is incorporated into a molar continuity equation, along with the required state equations, to form what is referred to here as the "Mole Model" for transport simulations. Equation (3-8) is generally incorporated into a mass continuity equation, along with required state equations, to form the common A-D model used for subsurface

transport simulations in hydrology and environmental science (e.g., Abriola and Pinder, 1985; Pruess, 1987; Falta *et al.*, 1989, 1992). To allow for simple direct comparisons between models here, equation (3-10), a molar-flux counterpart to equation (3-8) will be incorporated into a molar continuity equation referred to here as the "Mass Model." Other than the use of molar flux units, the Mass Model defined here is equivalent to the common A-D model used in hydrology and environmental science (i.e., it uses the same advective reference velocity).

It was suggested by Farr and McWhorter (1988) that the Darcy seepage velocity gives a macroscopic mole-average velocity (in keeping with the chemical engineering literature) and that equation (3-6), as part of the Mole Model, should be used to describe diffusion fluxes relative to the Darcy advective velocity. (As an aside, use of the Mole Model does linearize many transport problems because the total molar density, c, in equation (3-6) is a function of only pressure and temperature for an ideal gas, whereas the mass density in equation (3-8) is a function of composition as well.) However, the use of the Mole Model with the traditional form of Darcy's law appears incorrect for gaseous transport in light of the highly reproducible experimental observations supporting Graham's law of diffusion (Graham, 1833; Hoogschagen, 1953, 1955; Evans *et al.*, 1961a, 1962a, 1963; Wicke and Hugo, 1961; Wakao and

Smith, 1962; Rothfeld, 1963; Gunn and King, 1969; Remick and Geankopplis, 1973; Alzaydi, 1975, 1978).

These observations show that the ratio of countercurrent molar fluxes (relative to coordinates fixed on the porous medium) under isobaric, isothermal conditions is given by Graham's law of diffusion

$$\frac{N_A}{N_B} = \frac{-\sqrt{M_B}}{\sqrt{M_A}} \tag{3-16}$$

and this holds for all pressures and pore sizes (not just in the Knudsen regime). This is in contrast to the equimolar and equimass countercurrent diffusion predicted by the Mole and Mass Models, respectively. Thus, the Darcy seepage velocity represents neither a mass-average velocity nor a mole-average velocity.

In order to correctly utilize the traditional transport phenomena modeling framework (e.g., Bird *et al.*, 1960) to derive convenient gaseous diffusion equations for porous media transport modeling, the Darcy seepage velocity must be known in terms of a weighted average of species drift velocities (analogous to equations (3-3), (3-5), and (3-11)). This is addressed in the following section.

Identification of Graham-Average Velocity

Given one general form of the molecular diffusion equation, in specified flux units relative to a given advective velocity (e.g., equation (3-6)), alternate forms of the molecular diffusion equation in differing flux units

and/or referenced to differing advective velocities can be derived. Simply changing the flux units used in a given diffusion equation is easily accomplished; however, accounting for a change in the advective reference velocity can involve difficult algebraic manipulations.

The doctoral thesis of Clazie (1967) contains a concise, general statement of the traditional transport phenomena modeling framework for molecular diffusion, also discussed by Bird *et al.* (1960), Cussler (1976), and de Groot and Mazur (1962). Of particular interest here, Clazie (1967) derived equations for transforming between different forms of the diffusion equation. Clazie's work also provides the basis for deriving or, more aptly, "identifying" the meaning of the Darcy seepage velocity in terms of species drift velocities. Clazie's most general transformation equation is, for an n-species mixture

$$\mathcal{J}_i^{FR} = \frac{\xi_i^F}{\xi_i^{F'}} \mathcal{J}_i^{F'R'} - \left[\frac{\xi_i^F}{\xi^R} \sum_{j=1}^{n} \frac{\xi_j^R}{\xi_j^{F'}} \mathcal{J}_j^{F'R'} \right] \tag{3-17}$$

where ξ_i^R and ξ^R are reference frame weighting factors defined by

$$\mathbf{v}^R = \frac{\sum \xi_i^R \mathbf{v}_i}{\sum \xi_i^R} \tag{3-18}$$

and

$$\xi^R = \sum \xi_i^R \tag{3-19}$$

The double superscript *FR* on the flux symbols of equation (3-17) indicates that the species *i* flux is an

"*F*-flux" relative to an "*R*-average velocity." *F* and *R* can take on the symbols *M*, *N*, *V*, or any other letter to indicate mass, molar, volume, or other type of flux or advective reference velocity, respectively. The prime symbols used in the superscripts (e.g., *F′*, *R′*) indicate that the flux type or advective reference velocity is associated with an alternate diffusion equation. The primed superscripts on the right-hand side of equation (3-17) are associated with the known or given diffusion equation, while the unprimed superscripts on the left-hand side of equation (3-17) are associated with the unknown diffusion equation.

Equation (3-18) describes the advective reference velocity, and it has the same form as equations (3-3), (3-5), and (3-11). The applicable reference frame weighting factors for use in equation (3-17) can be determined by direct comparison of equation (3-18) with defined advective reference velocity equations, such as equations (3-3), (3-5), and (3-11). For reference purposes, the weighting factors for the three reference frames discussed thus far are listed in Table 3-1.

Table 3-1. Reference frame weighting factor, ξ_i^R

Reference frame	R	ξ_i^R	ξ^R
Mass-average velocity	M	ρ_i	ρ
Mole-average velocity	N	c_i	c
Volume-average velocity	V	$c_i V_i$	1

The flux unit factors, ξ_i^F and ξ^F are defined by

$$\mathcal{J}_i^{FR} = \xi_i^F(\mathbf{v}_i - \mathbf{v}^R) \tag{3-20}$$

and

$$\xi^F = \sum \xi_i^F \tag{3-21}$$

Equation (3-20) is of the same form as equations (3-2), (3-4), and (3-12), and the flux unit factors can be determined by direct comparison of these equations. For reference purposes, flux unit factors for mass and molar fluxes are listed in Table 3-2.

Table 3-2. Flux unit factor, ξ_i^F

Type of flux	F	ξ_i^F	ξ^F
Mass flux	M	ρ_i	ρ
Molar flux	N	c_i	c

Clazie (1967) also showed that

$$\sum \frac{\xi_i^R}{\xi_i^F}\mathcal{J}_i^{FR} = 0 \tag{3-22}$$

This equation indicates that the sum of species diffusion fluxes in a phase equals zero only when the units of flux and the reference velocity directly correspond (e.g., mass flux relative to a mass-average velocity), as mentioned previously. In such cases, the reference frame weighting factor and the flux unit factor in equation (3-22) are equivalent (Tables 3-1 and 3-2).

As shown below, Graham's law of diffusion, equation (3-16), can be written in the same form as equation (3-22), thus providing for the identification of the applicable reference frame weighting factor and flux unit factor required to define the Darcy seepage velocity in terms of species drift velocities. Because the Darcy seepage velocity has been shown to be neither a mass-average nor a mole-average velocity, and because it is most convenient to use either mass or molar flux units in practical transport models, it is apparent that the species diffusion fluxes relative to the Darcy seepage velocity will not sum to zero for the gas phase. The sum of diffusion fluxes will be given by equation (3-22), where the proper weighting factors ξ_i^R and ξ_i^F have yet to be identified. Once ξ_i^R is known, equation (3-18) will be used to define the Darcy advective reference velocity.

Graham's law of diffusion, equation (3-16), can be rewritten as

$$\sqrt{M_A}\boldsymbol{N}_A + \sqrt{M_B}\boldsymbol{N}_B = 0 \qquad (3\text{-}23)$$

with the multicomponent generalization

$$\sum \sqrt{M_i}\boldsymbol{N}_i = 0 \qquad (3\text{-}24)$$

In the isobaric case, no viscous flux (or flux that dissipates momentum) occurs, and the Darcy velocity representing viscous flux is zero. In this case, the diffusion fluxes, referred to here as $\mathbf{J}_i^{NG}$ are equivalent to fluxes relative to fixed coordinates $\mathbf{N}_i$, and equation (3-24)

is equivalent to equation (3-22). This equivalence allows us to identify the weighting factors ξ_i^R and ξ_i^F that are necessary to define the Darcy seepage velocity in terms of species drift velocities. The ratio ξ_i^R/ξ_i^F in equation (3-22) is given by

$$\frac{\xi_i^R}{\xi_i^F} = \sqrt{M_i} \tag{3-25}$$

Because equation (3-24) is expressed in terms of molar fluxes,

$$\xi_i^F = \xi_i^N = c_i \tag{3-26}$$

and

$$\xi_i^R = \sqrt{M_i} c_i \tag{3-27}$$

This reference frame weighting factor will be designated with the superscript G, and the corresponding weighted average of species drift velocities is

$$\mathbf{v}^G = \frac{\sum \xi_i^G \mathbf{v}_i}{\sum \xi_i^G} = \frac{\sum \sqrt{M_i} c_i \mathbf{v}_i}{\sum \sqrt{M_i} c_i} \tag{3-28}$$

By multiplying each term in both the numerator and denominator by M_i/M_i, equation (3-28) can be written alternatively as

$$\mathbf{v}^G = \frac{\sum M_i^{-\frac{1}{2}} \rho_i \mathbf{v}_i}{\sum M_i^{-\frac{1}{2}} \rho_i} \tag{3-29}$$

The reference velocity of equations (3-28) and (3-29) will be referred to as the Graham-average velocity, in

recognition of the much overlooked work of Thomas Graham between 1828 and 1833, and the superscript G will be used to reflect this. As shown later in the Hydrodynamic Analysis Section, when equations (3-28) and (3-29) are used to describe advective flux macroscopically, they yield a velocity that corresponds directly to the viscous flux. In porous media, the viscous flux is given by Darcy's law. In tube or capillary flow, the viscous flux is given by Poiseuille's law.

Derivation of Diffusion-Flux Equations

Now that the Graham-average velocity has been defined in terms of species drift velocities, diffusion-flux equations referenced to the Graham-average velocity can be derived. Given the diffusion flux relative to one reference velocity, (e.g., from equation (3-6)), equation (3-17) can be used to derive the diffusion flux relative to the Graham-average velocity. To transform equation (3-6) into a molar flux relative to the Graham-average velocity, equation (3-17) becomes

$$\mathcal{J}_A^{NG} = \mathcal{J}_A^{NN} - \frac{C_A}{\sqrt{M_A}C_A + \sqrt{M_B}C_B}\left[\frac{\sqrt{M_A}C_A}{C_A}\mathcal{J}_A^{NN} + \frac{\sqrt{M_B}C_B}{C_B}\mathcal{J}_B^{NN}\right] \qquad (3\text{-}30)$$

for the flux of species A in a binary case. Equation (3-30) can be reduced to

$$J_A^{NG} = -\left[1 + \frac{C_A\left(\sqrt{M_B} - \sqrt{M_A}\right)}{\sqrt{M_A}C_A + \sqrt{M_B}C_B}\right] cD_{AB}^{*}\nabla\chi_A \qquad (3\text{-}31)$$

The second flux term on the right-hand side of equation (3-31) represents the difference between this new diffusion flux equation and the common equation (3-6). The second term in equation (3-31) will be of the same sign as the first term only when species *A* is the lighter molecular mass species in the mixture. The second term will be of opposite sign for the higher molecular mass species, thus reducing the net diffusive species flux from that given by the first term (or equation (3-6)). Also, it should be noted that the second term in equation (3-31) vanishes when the molecular masses of the species are equal, making equations (3-6) and (3-31) equivalent for this special case.

Equation (3-31) can be further reduced to give

$$J_A^{NG} = -\left[\frac{\sqrt{M_B}}{\sqrt{M_A}\chi_A + \sqrt{M_B}\chi_B}\right] cD_{AB}^{*}\nabla\chi_A \qquad (3\text{-}32)$$

and the flux of species *B* is given by

$$J_B^{NG} = -\left[\frac{\sqrt{M_A}}{\sqrt{M_A}\chi_A + \sqrt{M_B}\chi_B}\right] cD_{BA}^{*}\nabla\chi_B \qquad (3\text{-}33)$$

The corresponding equations for mass diffusion fluxes are

$$J_A^{MG} = -\left[\frac{M_B^{-\frac{1}{2}}}{M_A^{-\frac{1}{2}}\omega_A + M_B^{-\frac{1}{2}}\omega_B}\right] \rho D_{AB}^{*}\nabla\omega_A \qquad (3\text{-}34)$$

and

$$\mathcal{J}_B^{MG} = -\left[\frac{M_A^{-\frac{1}{2}}}{M_A^{-\frac{1}{2}}\omega_A + M_B^{-\frac{1}{2}}\omega_B}\right]\rho D_{BA}^{*}\nabla\omega_B \qquad (3\text{-}35)$$

These new diffusion equations, as used in the general continuity equations presented later in this chapter (which use Darcy's law for the advective terms) comprise what will be referred to here as the Graham Model.

Theoretical Support For Graham Model

This section is divided into two parts, containing support for the Graham Model by direct comparisons to the DGM and the diffusive-slip flux model of Kramers and Kistemaker (1943).

Comparison to the Dusty-Gas Model

Results from the DGM support the contention that equations (3-28) and (3-29) represent the reference velocity corresponding to the Darcy seepage velocity and thus, that equations (3-32) through (3-35) are the correct diffusion flux equations to use in combination with Darcy's law for cases where the molecular diffusion regime prevails (i.e., in porous media in which Knudsen and Klinkenberg effects are negligible). The following equation for the "total diffusive bulk flux" or the "nonequimolar flux" of the gas phase can be distilled from the DGM, assuming that forced, temperature, and pressure diffusion are negligible:

$$\mathbf{N}^D = (1-\Delta'_{AB})^{-1}\left[\frac{\sqrt{M_A} - \sqrt{M_B}}{\sqrt{M_A}\chi_A + \sqrt{M_B}\chi_B}\right] cD^*_{AB}\nabla\chi_A \qquad (3\text{-}36)$$

Equation (3-36) is the molar-flux equivalent to Cunningham and Williams' (1980) Equation (4.65), where Δ'_{AB} is a factor which modifies the diffusion coefficient to meet the second-order approximation of the rigorous kinetic theory of gases (as given by the Burnett equations - see Hirschfelder *et al.*, 1954). This factor would be very small compared to unity for cases of interest in subsurface modeling. The second order approximation is necessary only when relative changes in the phase density, velocity, or temperature are large compared with unity over a mean-free-path distance (Hirschfelder *et al.*, 1954). Such conditions might arise in shock waves or nuclear reactors, but not in cases of interest here. Also, neglecting the second-order effects here is consistent with our previous assumption of negligible pressure and temperature diffusion, which are second-order effects. Thus, equation (3-36) becomes

$$\mathbf{N}^D = \left[\frac{\sqrt{M_A} - \sqrt{M_B}}{\sqrt{M_A}\chi_A + \sqrt{M_B}\chi_B}\right] cD^*_{AB}\nabla\chi_A \qquad (3\text{-}37)$$

The total diffusive or nonequimolar flux is the nonsegregative fluid flux caused by diffusive forces (i.e., concentration gradients), and it is simply the sum of diffusion fluxes for all species in the phase. The nonequimolar flux can also be defined by the following equation (Thorstenson and Pollock, 1989)

$$\mathbf{N}^D = \mathbf{N}^T - \mathbf{N}^V \tag{3-38}$$

where $\mathbf{N}^T$ is the total molar flux, given by the phase sum of species fluxes (i.e., the sum of $\mathbf{N}_i$ in equation (3-1); $\mathbf{N}^T = c\mathbf{v}^N$), and $\mathbf{N}^V$ is the viscous flux, given by Darcy's law. In contrast to the viscous flux given by Darcy's law, the nonequimolar flux results in zero net momentum transfer between the fluid and the porous medium walls. The species flux associated with the nonequimolar flux is added to the (segregative) diffusive species flux defined relative to the mole-average velocity (as given by equation (3-6)) to complete this simplified subset of the DGM (Cunningham and Williams, 1980; Thorstenson and Pollock, 1989). The "total diffusive species flux" is then given by (Thorstenson and Pollock, 1989)

$$\mathbf{N}_i^T = [\mathbf{N}_i^D] + \mathbf{N}_i^V = [\mathbf{J}_i^{NN} + \chi_i \mathbf{N}^D] + \chi_i \mathbf{N}^V \tag{3-39}$$

To solve for $\mathbf{N}_i^D$ as indicated by equation (3-39), equation (3-37) is multiplied by the mole fraction of a given species (say species A in binary mixture) and that result is added to the molar diffusion flux relative to a mole-average velocity (from equation (3-6)), giving

$$\mathbf{N}_A^D = -cD_{AB}^* \nabla \chi_A + \left[\frac{\chi_A \left(\sqrt{M_A} - \sqrt{M_B} \right)}{\sqrt{M_A}\chi_A + \sqrt{M_B}\chi_B} \right] cD_{AB}^* \nabla \chi_A = \mathbf{J}_A^{NG} \tag{3-40}$$

Upon simple rearrangement, this is equivalent to equation (3-31), which is indicated by the RHS of equation (3-40).

Thus, the DGM results are equivalent to those derived in this dissertation, even though the DGM is derived in a different manner. Because the DGM has been verified against experimental data and it is widely accepted, this equivalence provides firm support to the contention made here that diffusive fluxes should be referenced to the "Graham-average" velocity (equation [3-28] or [3-29]) when using Darcy's law or Poiseuille's law to represent advection. In the following section, additional support for this contention is provided using hydrodynamic arguments, combining a modified Poiseuille's solution for transport of gas mixtures in capillaries with the bundle-of-tubes analogy for transport in porous media.

Hydrodynamic Analysis

This section is presented primarily to provide additional support for the Graham Model, as derived previously. However, the presentation that follows can also be viewed as a second derivation of the Graham Model (in alternative form), using a completely different approach than that previous given in this chapter.

As many previous investigators have noted, a direct analogy can be drawn between flow in tubes or capillaries and flow in porous media. The tractable geometry of a tube allows for direct solution of the Navier-Stokes equation, and this solution describes the steady mass-average velocity field across the tube. Using the traditional non-slip

boundary condition, $v^{M}_{(r=a)} = 0$, the classic Poiseuille solution for the velocity field in a horizontal tube is derived

$$\mathbf{v}^{M}_{(r)} = \frac{-1}{4\mu}\frac{dP}{dx}(a^2 - r^2) \qquad (3\text{-}41)$$

where r is the radial coordinate measured outward from the center of the tube, a is the radius of the tube, x is the coordinate measured along the axis of the tube, and μ is the dynamic fluid viscosity. The analogy between tube flow and porous media flow is powerful because after integrating equation (3-41) over the tube cross section, an expression for the total molar flow rate over the cross-sectional area of the tube results which has the same form as Darcy's law. This expression is commonly referred to as Poiseuille's law,

$$\tilde{\boldsymbol{N}} = \frac{-a^2 P}{8\mu RT}\frac{dP}{dx} \qquad (3\text{-}42)$$

which differs from Darcy's law only in the "geometric factor". The geometric factor, $a^2/8$, in Poiseuille's law corresponds directly to the permeability, $\boldsymbol{k}$, in Darcy's law. The effects of porous media flow-path tortuosity are included in the permeability parameter. Exchanging geometric factors according to the bundle-of-tubes analogy, equation (3-42) converts to Darcy's law for horizontal molar flux.

The non-slip boundary condition used in the derivation of Poiseuille's law has been widely considered applicable to gas transport so long as the tube diameter greatly exceeds

the mean free path of gas molecules. While this is true for a pure gas, the classic non-slip boundary condition is not valid when species of differing molecular mass are diffusing. In the absence of a pressure gradient, equation (3-41) gives $v^M = 0$, which has already been shown to be incorrect for cases where gaseous species of differing molecular mass are interdiffusing.

Using momentum transfer arguments and the kinetic theory of gases, Kramers and Kistemaker (1943) first showed that a diffusive-slip boundary condition for the mass-average velocity in such mixtures was required for correct solutions to this problem. Later, Hoogschagen (1953) experimentally rediscovered Graham's law of diffusion, which supported the arguments of Kramer and Kistemaker (1943). None of these investigators seemed to be aware of Graham's experimental work (circa 1830), which first illuminated this transport behavior.

Jackson (1977) used the diffusive-slip boundary condition first presented by Kramers and Kistemaker (1943) to derive a modified, multicomponent Poiseuille solution for the mass-average velocity field in a tube (in the molecular diffusion regime). Using the notation adopted in this dissertation, the appropriate diffusive-slip boundary condition given by Jackson (1977) is equivalent to

$$\mathbf{v}^{M}_{(r=a)} = \frac{-\sum\sqrt{M_i}\mathbf{J}^{NM}_{i(r=a)}}{\sum\sqrt{M_i}c_i} \qquad (3\text{-}43)$$

where the $\mathbf{J}_i^{NM}{}_{(r=a)}$ represent local or microscopic diffusive fluxes at the boundary. The diffusive-slip boundary condition given in equation (3-43) for the mass-average velocity can be expressed alternatively as a non-slip boundary condition for the Graham-average velocity, $\mathbf{v}^{G}$. Using the definition of the molar diffusion flux relative to a mass-average velocity ($\mathbf{J}_i^{NM}$), the RHS of equation (3-43) can be expanded to show that

$$\mathbf{v}^{M}_{(r=a)} = \frac{-\sum\sqrt{M_i}c_i\left(\mathbf{v}_{i(r=a)} - \mathbf{v}^{M}_{(r=a)}\right)}{\sum\sqrt{M_i}c_i} \qquad (3\text{-}44)$$

where $\mathbf{v}_{i(r=a)}$ are the species drift velocities at the boundary. Separating the terms in the RHS of equation (3-44) gives

$$\mathbf{v}^{M}_{(r=a)} = \mathbf{v}^{M}_{(r=a)} - \frac{\sum\sqrt{M_i}c_i\mathbf{v}_{i(r=a)}}{\sum\sqrt{M_i}c_i} \qquad (3\text{-}45)$$

The last term on the RHS of equation (3-45) is, by definition, the Graham-average velocity (see equation (3-28)), and to satisfy equation (3-45), the Graham-average velocity must be zero. Thus, the Graham-average velocity must vanish at the boundary. As mentioned previously, in the special case where the species of a gas mixture have identical molecular masses, the Graham-average velocity equals the mass-average velocity.

Using the diffusive-slip boundary condition for the mass-average velocity shown in equation (3-43), or the equivalent non-slip boundary condition for the Graham-average velocity, a modified form of the Poiseuille solution results

$$\mathbf{v}^{M}_{(r)} - \mathbf{v}^{M}_{(r=a)} = \mathbf{v}^{G}_{(r)} = \frac{-1}{4\mu}\frac{dP}{dx}(a^2 - r^2) \qquad (3\text{-}46)$$

The use of the bundle-of-tubes analogy seems justified for the case where diffusive slip occurs, just as it does for the case of a pure fluid (Feng and Stewart, 1973; Alzaydi *et al.*, 1978). Integrating equation (3-46), using the boundary condition given by equation (3-43), yields a modified form of Poiseuille's law, analogous to a modified form of Darcy's law, accounting for diffusive slip along the porous media walls. In terms of the integrated total molar flux of the gas phase over the tube cross-section, Jackson (1977) writes the modified Poiseuille's law as

$$\tilde{N} = \frac{-a^2 P}{8\mu RT}\frac{dP}{dx} - \frac{\Sigma\sqrt{M_i}\tilde{J}_i^{NN}}{\Sigma\sqrt{M_i}\chi_i} \qquad (3\text{-}47)$$

where $\tilde{J}_i^{NN}$ is the (macroscopic) integrated average of diffusive flux over the tube cross-section.

The first term on the RHS of equation (3-47) represents the viscous flux, while the second term represents the diffusive-slip or nonequimolar flux. Exchanging geometric factors according to the bundle-of-tubes analogy, equation (3-47) converts to a modified form of Darcy's law. If the modified forms of Poiseuille's law or Darcy's law are used

to represent advection in an A-D model, then the diffusive flux relative to a mole-average velocity ($\mathbf{J}_i^{NN}$) must be used to represent the nonadvective terms. For most purposes, however, it is preferable to use the modified diffusion equations (equations [3-32] through [3-35]) and retain the traditional forms of Poiseuille's law and Darcy's law for A-D models. This is because the traditional forms of Poiseuille's law and Darcy's law represent the viscous flux driven by pressure gradients, and the modified diffusion equations account for the entire flux driven by gradients in gas composition.

Because $\tilde{\mathbf{N}} = c\tilde{\boldsymbol{\nu}}^N$, and for an ideal gas, $c = P/RT$ (where R and T represent the universal gas constant and absolute temperature), equation (3-47) can be written in terms of the macroscopic mole-average velocity:

$$\frac{-a^2}{8\mu}\frac{dP}{dx} = \tilde{\mathbf{v}}^N + \frac{\Sigma\sqrt{M_i}\tilde{\mathbf{J}}_i^{NN}}{\Sigma\sqrt{M_i}c_i} \qquad (3\text{-}48)$$

Because $\tilde{\mathbf{J}}_i^{NN} = \tilde{\mathbf{N}}_i - c_i\tilde{\boldsymbol{\nu}}^N$, equation (3-48) can be expressed as

$$\frac{-a^2}{8\mu}\frac{dP}{dx} = \tilde{\mathbf{v}}^N + \frac{\Sigma\sqrt{M_i}(\tilde{\mathbf{N}}_i - c_i\tilde{\mathbf{v}}^N)}{\Sigma\sqrt{M_i}c_i} \qquad (3\text{-}49)$$

which reduces to

$$\frac{-a^2}{8\mu}\frac{dP}{dx} = \frac{\Sigma\sqrt{M_i}\tilde{\mathbf{N}}_i}{\Sigma\sqrt{M_i}c_i} \qquad (3\text{-}50)$$

Dropping the tilde symbols to complete the transition to macroscopic equations, and recognizing that $\mathbf{N}_i = c_i\boldsymbol{\nu}_i$, the

right-hand side of equation (3-50) equals the Graham-average velocity (equation [3-28]), thus supporting the use of equations (3-32) through (3-35) for diffusive fluxes in tubes when the traditional form of Poiseuille's law is used to represent advection. Using the bundle-of-tubes analogy, support is also provided for the use of equations (3-32) through (3-35) for diffusive fluxes in porous media when the traditional form of Darcy's law is used to represent advection.

The *effective* diffusion coefficients used in equations (3-32) through (3-35) differ significantly, of course, depending on whether these equations are being used to model transport in tubes or porous media, where porosity and tortuosity factors must be used. Because the permeability parameter used in Darcy's law does not include the "blockage" effects of porosity on species drift velocities, both sides of equation (3-50) must be divided by the gas-filled porosity to obtain porous media equivalent of equation (3-50), which shows that the macroscopic advective velocity (the Darcy seepage velocity) commonly used in subsurface transport modeling, v_s, equals the Graham-average velocity

$$\mathbf{v}_s = \frac{\mathbf{q}}{\theta_g} = \frac{-\mathbf{k}}{\mu\theta_g}\frac{dP}{dx} = \frac{\sum\sqrt{M_i}c_i\mathbf{v}_i}{\sum\sqrt{M_i}c_i} = \mathbf{v}^G \qquad (3\text{-}51)$$

Formulation of Continuity Equations

Molar and mass continuity equations for the gas phase in porous media, incorporating the new diffusive-flux equations, will now be presented. These continuity equations comprise the Graham Model, and they can be used to replace their traditional counterparts in multi-phase, multi-component subsurface transport models. The advective transport terms retain their standard form, using the traditional form of Darcy's law. The modifications to traditional A-D transport models have all been incorporated into the modified diffusion-flux equations of the Graham Model. As alluded to previously, alternative continuity equations could be formed using the traditional equations for molecular diffusion flux (e.g., equation (3-6)) along with a modified form of Darcy's law, analogous to the modified Poiseuille's law shown in equation (3-47).

Continuity equations are only presented for the binary case, because in general the diffusion-flux equations derived here are only valid for binary systems. However, if anticipated multi-component effects within the gas phase are small (i.e., if the species flux of interest is not expected to be significantly affected by, and affected in different ways by the concentration gradients of other species in the mixture), then the binary version of the Graham Model presented here can be applied to multi-component systems by placing the existing species into two groups. This approach should yield acceptable results for many cases involving

transport of volatile organic compounds in subsurface air, where the gas components (including N_2, O_2, CO_2, and H_2O) can be grouped together as "air" (Bird *et al.*, 1960; Cussler, 1976). Care should be taken in ignoring multicomponent effects, however, as they may be significant in the root zone or in sanitary land fills, where gas production may produce composition gradients for CO_2 and CH_4 that are quite different than those for N_2, O_2, and H_2O (Thorstenson and Pollock, 1989).

It is generally more convenient to use molar, rather than mass, continuity equations for modeling gaseous transport in porous media. However, because mass continuity equations may prove convenient in certain applications, they are also presented here. The general molar continuity equations for binary gaseous species *A* and *B* in porous media are

$$\frac{\partial}{\partial t}(c_A\theta_g) = -\nabla \cdot \boldsymbol{N}_A + R_A + E_A \qquad (3\text{-}52)$$

and

$$\frac{\partial}{\partial t}(c_B\theta_g) = -\nabla \cdot \boldsymbol{N}_B + R_B \qquad (3\text{-}53)$$

where R_A and R_B are molar reaction rates, and E_A is the interphase molar transfer rate. Species *A* is taken as condensible (say a volatile organic compound) and species *B* is taken as non-condensible (say air). Thus, the interphase transfer rate for species *B* is neglected. The sum of

equations (3-52) and (3-53) forms the molar continuity equation for the gas phase

$$\frac{\partial}{\partial t}(c\,\theta_g) = -\nabla \cdot \boldsymbol{N} + (R_A + R_B) + E_A \qquad (3\text{-}54)$$

Note that the species reaction rates do not generally sum to zero on a molar basis. To complete the Graham Model using equations (3-52) through (3-54), $\mathbf{N}_i = \chi_i c\mathbf{q} + \mathbf{J}_i^{NG}$ and $\mathbf{N} = c\mathbf{q} + (\mathbf{J}_A^{NG} + \mathbf{J}_B^{NG})$, where $\mathbf{q}$ is the Darcy volume flux. In the Graham Model, the diffusion fluxes sum to zero only in the special case where the species molecular masses are equal.

Adding the diffusive fluxes given by equations (3-32), (3-6), and (3-10) to the viscous flux, the species *A* molar fluxes given by the Graham, Mole, and Mass Models are shown below in equations (3-55), (3-56), and (3-57), respectively

$$\boldsymbol{N}_A^G = \chi_A c\boldsymbol{q} - \left[\frac{\sqrt{M_B}}{\sqrt{M_A}\chi_A + \sqrt{M_B}\chi_B}\right] cD_{AB}^*\nabla\chi_A \qquad (3\text{-}55)$$

$$\boldsymbol{N}_A^N = \chi_A c\boldsymbol{q} - cD_{AB}^*\nabla\chi_A \qquad (3\text{-}56)$$

$$\boldsymbol{N}_A^M = \chi_A c\boldsymbol{q} - \left[\frac{M_B}{M_A\chi_A + M_B\chi_B}\right] cD_{AB}^*\nabla\chi_A \qquad (3\text{-}57)$$

Inserting equation (3-55) into equations (3-52) through (3-54) yields the continuity equations (3-58) through (3-60) below for the Graham Model

$$\frac{\partial}{\partial t}(c_A\theta_g) = -\nabla\cdot\left[c_A\boldsymbol{q} - \left(\frac{\sqrt{M_B}}{\sqrt{M_A}\chi_A+\sqrt{M_B}\chi_B}\right) cD^*_{AB}\nabla\chi_A\right] + R_A + E_A \qquad (3\text{-}58)$$

$$\frac{\partial}{\partial t}(c_B\theta_g) = -\nabla\cdot\left[c_B\boldsymbol{q} - \left(\frac{\sqrt{M_A}}{\sqrt{M_A}\chi_A+\sqrt{M_B}\chi_B}\right) cD^*_{BA}\nabla\chi_B\right] + R_B \qquad (3\text{-}59)$$

$$\frac{\partial}{\partial t}(c\,\theta_g) = -\nabla\cdot\left[c\,\boldsymbol{q} + \left(\frac{\sqrt{M_A}-\sqrt{M_B}}{\sqrt{M_A}\chi_A+\sqrt{M_B}\chi_B}\right) cD^*_{AB}\nabla\chi_A\right] + (R_A+R_B) + E_A \qquad (3\text{-}60)$$

The second term on the RHS of equation (3-60) is the nonequimolar flux, resulting from the sum of species diffusion fluxes. The viscous volume flux for all three models is given by Darcy's law

$$\boldsymbol{q} = -\frac{\boldsymbol{k}}{\mu}(\nabla P - \rho\boldsymbol{g}) \qquad (3\text{-}61)$$

The second term in equation (3-61) describes the component of viscous flux driven by gravitational force. Although this dissertation does not generally discuss this component of the viscous flux, Thorstenson and Pollock (1989) concluded that the form and predicted behavior of the DGM remained unchanged in the presence of a gravitational field. They also showed that Graham's law of diffusion, described here as applicable to the isobaric case, is also applicable to a gas mixture at hydrostatic equilibrium in a gravitational field. When fluid density depends on composition, a combined pressure and gravitational potential can not be defined (Hubbert, 1940; Corey and Kemper, 1961; Corey and Klute, 1985). It is therefore important to keep

the pressure gradient and gravitational force terms separate in general modeling formulations.

The Graham Model mass continuity equations for binary gaseous species *A* and *B* are

$$\frac{\partial}{\partial t}(\rho_A \theta_g) = -\nabla \cdot \left[\rho_A \boldsymbol{q} - \left(\frac{M_B^{-\frac{1}{2}}}{M_A^{-\frac{1}{2}} \omega_A + M_B^{-\frac{1}{2}} \omega_B} \right) \rho D_{AB}^* \nabla \omega_A \right] + r_A + e_A \qquad (3\text{-}62)$$

and

$$\frac{\partial}{\partial t}(\rho_B \theta_g) = -\nabla \cdot \left[\rho_B \boldsymbol{q} - \left(\frac{M_A^{-\frac{1}{2}}}{M_A^{-\frac{1}{2}} \omega_A + M_B^{-\frac{1}{2}} \omega_B} \right) \rho D_{BA}^* \nabla \omega_B \right] + r_B \qquad (3\text{-}63)$$

where r_A and r_B are mass reaction rates and e_A is the interphase mass transfer rate of condensible species *A*. Equations (3-62) and (3-63) sum to give

$$\frac{\partial}{\partial t}(\rho \theta_g) = -\nabla \cdot \left[\rho \boldsymbol{q} + \left(\frac{M_A^{-\frac{1}{2}} - M_B^{-\frac{1}{2}}}{M_A^{-\frac{1}{2}} \omega_A + M_B^{-\frac{1}{2}} \omega_B} \right) \rho D_{AB}^* \nabla \omega_A \right] + e_A \qquad (3\text{-}64)$$

Note that the species reaction rates always sum to zero on a mass basis, although this does not represent a true simplification compared to the molar continuity equations. If a reaction results in a net change in total moles, the Darcy flux will be influenced, and this influence is more directly shown by equation (3-60) than equation (3-64). Direct coupling between the continuity equation and the equation of motion (Darcy's law) is essential, not only because of the possibility of reaction-driven advection, but also because interphase transfer (evaporation/condensation)

can drive advection in the gas phase. This has only been recognized recently in the hydrologic literature (Falta *et al.*, 1989; Mendoza and Frind, 1990). Equation (3-60) is somewhat easier to couple with Darcy's law because the total molar density, c, in the viscous flux term is simply given by the ideal gas law (for ideal gases), whereas the mass density in the viscous flux term of equation (3-64) is a function of composition as well as pressure and temperature. Thus, the model based on molar continuity equations is simpler because molar state equations are simpler than mass state equations for an ideal gas. For reference, the mass state equation required when coupling equation (3-64) to Darcy's law is

$$\rho = c_A M_A + c_B M_B = c(\chi_A M_A + \chi_B M_B) \qquad (3\text{-}65)$$

The differences in predicted transport behavior between the Graham Model and existing A-D models are most pronounced under isobaric or nearly isobaric conditions, where diffusive fluxes dominate. In cases dominated by viscous flux, the differences in model-predicted diffusion fluxes can be obscured by the magnitude of viscous fluxes.

Under the nearly isobaric conditions where diffusive fluxes dominate, the local equilibrium assumption for interphase partitioning seems justified. Thus, we will assume that Raoult's law or Henry's law suffices for determining the gaseous concentrations of our condensible species *A* in the presence of a nonaqueous phase liquid (NAPL) or a contaminated aqueous phase, respectively. Both

Henry's "constant" and vapor pressure are significantly dependent on temperature, so if the transport model is to properly account for the effects of temperature changes, it is important that both these quantities be specified as functions of temperature. Because the dimensional Henry's constant is divided by RT to obtain a dimensionless partition coefficient, gas-phase partitioning is shown to decrease with increasing temperature in models failing to represent the temperature dependence of Henry's constant (e.g., Bonazountas and Wagner, 1984).

To obtain the most general transport modeling results, the gas viscosity should be represented as a function of composition and temperature (Buddenberg and Wilke, 1949; Wilke, 1950; Hirschfelder *et al.*, 1954), and the binary diffusion coefficients should be represented as functions of pressure and temperature (Bird *et al.*, 1960). If the model is to be used with effective multicomponent diffusion coefficients (for ternary mixtures where such coefficients allow the use of a binary diffusion formulation; see Bird *et al.*, 1960; Cussler, 1976), then these diffusion coefficients will, of course, need to be represented as functions of gas composition, as well as pressure and temperature.

CHAPTER 4

ANALYTICAL COMPARISONS OF MODELS

In this Chapter, comparisons are made of model-predicted, steady-state molecular diffusion fluxes and binary flux ratios under isobaric, isothermal conditions in porous media. These comparisons are made to evaluate differences between the Graham Model and traditional A-D transport models. Diffusion fluxes given by the Mole, Mass, and Graham Models are compared using analytical solutions for steady gas composition distributions under isobaric conditions using equations (3-6), (3-10), and (3-32), respectively. The steady-state diffusion flux for each respective model is calculated by evaluating the mole-fraction derivative using the respective model's analytical solution for the axial distribution of gas composition in a horizontal porous medium column with fixed boundary conditions. As shown in Chapter 3, the Graham Model is equivalent to the DGM for the molecular diffusion regime, given isothermal conditions and negligible pressure diffusion. The Graham Model is therefore taken as the standard against which the other two models are compared.

The steady-state countercurrent diffusion fluxes are computed for a horizontal porous medium column, similar to

that described in the thought experiment of Chapter 2, except that the porous medium column considered here is open-ended. The column considered in Chapter 2 is closed-ended, and pressure gradients exist during countercurrent transport of differing molecular mass species in closed systems. In contrast, the results derived below are based on the assumption that no pressure gradients exist in the column. To assure this, the column ends must be open to manifolds capable of maintaining constant pressure and gas composition.

Comparison of Steady Diffusion Flux Ratios

It is instructive to examine the isobaric binary flux ratios predicted by the three models. Because no viscous (or Darcy) flux occurs in the isobaric case, the model-predicted flux ratios can be easily determined by forming appropriate ratios using the diffusion flux equations. Recognizing that $\nabla\chi_B = -\nabla\chi_A$, the ratio formed by dividing equation (3-32) by equation (3-33) confirms that the Graham Model faithfully reproduces the behavior described by Graham's law, expressed in terms of a ratio of molar fluxes

$$\frac{J_A^{NG}}{J_B^{NG}} = \frac{N_A^G}{N_B^G} = \frac{-\sqrt{M_B}}{\sqrt{M_A}} \qquad (4\text{-}1)$$

Similarly, $\nabla\omega_B = -\nabla\omega_A$, and the ratio formed by dividing equation (3-34) equation (3-35) gives the ratio of mass fluxes predicted by the Graham Model

$$\frac{J_A^{MG}}{J_B^{MG}} = \frac{n_A^G}{n_B^G} = \frac{-\sqrt{M_A}}{\sqrt{M_B}} \qquad (4\text{-}2)$$

The Mole Model predicts equimolar countercurrent diffusion fluxes, which is readily seen by taking a ratio of equation (3-6) and its binary counterpart to give

$$\frac{J_A^{NN}}{J_B^{NN}} = \frac{N_A^N}{N_B^N} = -1 \qquad (4\text{-}3)$$

Dividing equation (3-14) by its binary counterpart gives the mass flux ratio predicted by the Mole Model

$$\frac{J_A^{MN}}{J_B^{MN}} = \frac{n_A^N}{n_B^N} = \frac{-M_A}{M_B} \qquad (4\text{-}4)$$

Dividing equation (3-8) by its binary counterpart shows that the Mass Model predicts equimass countercurrent diffusion

$$\frac{J_A^{MM}}{J_B^{MM}} = \frac{n_A^M}{n_B^M} = -1 \qquad (4\text{-}5)$$

Finally, dividing equation (3-10) by its binary counterpart shows that the Mass Model predicts a molar flux ratio of

$$\frac{J_A^{NM}}{J_B^{NM}} = \frac{N_A^M}{N_B^M} = \frac{-M_B}{M_A} \qquad (4\text{-}6)$$

As a dramatic example of the differences in predicted flux ratios given by the three models, consider the isobaric countercurrent diffusion of argon and helium in an open-ended column, as shown in Figure 4-1. Because argon and helium are gases at typical environmental conditions, they can occur in any mole fraction, and the difference in

molecular masses (M_{He} = 4.003 and M_{Ar} = 39.95) results in a range of gas density from 0.1664 to 1.661 g/L at 20° C and 1 atmosphere. Figure 4-1 shows the limiting case, where pure helium (species *A*) exists at the left-hand end of the column, and pure argon (species *B*) exists at the right-hand end of the column. Although the limiting case (with maximum concentration gradients) is shown in Figure 4-1, the analysis of flux ratios presented here holds for all cases. As readily seen by inspection of equations (4-1) through (4-6), isobaric diffusion flux ratios depend only on the molecular masses of the species involved.

For isobaric countercurrent diffusion of argon and helium, Table 4-1 shows the significant differences in model-predicted flux ratios. Table 4-1 also shows the significant differences in model-predicted isobaric flux ratios for a binary system of moist air (M_{air} = 28.7 g/mole) and tetrachloroethylene (PCE, M_{PCE} = 165.8 g/mole). This type of gas system is of great interest in the analysis of environmental problems involving solvent vapors in the subsurface.

Table 4-1. Comparison of model-predicted countercurrent flux ratios under steady, isobaric conditions

A-D model	Eqn. No.	$\mathbf{N}_{He}/\mathbf{N}_{Ar}$	$\mathbf{N}_{air}/\mathbf{N}_{PCE}$
Mole Model	(4-3)	-1	-1
Graham Model	(4-1)	-3.16	-2.40
Mass Model	(4-6)	-9.98	-5.78

Countercurrent diffusion of argon and helium through porous graphite is a problem of practical interest in the design of nuclear reactors. Thus, this type of problem has been studied in detail, both theoretically and experimentally (e.g., Evans et al., 1961a,b, 1962a,b, 1963; Mason et al., 1967). In fact, the Dusty Gas Model (DGM) was developed to explain the transport behavior associated with this type of problem. In Chapter 5, the three transport models are compared directly to experimental data for countercurrent transport of helium and argon in porous graphite. Of the three models, it is shown that only the Graham Model adequately represents the processes active during the experiments of Evans et al. (1961a).

Comparison of Steady-State Fluxes

Three examples of steady, countercurrent diffusion are provided to highlight the differences in model predicted fluxes. The first two examples involve vapor diffusion, and the third example involves gas diffusion. The differences in model-predicted fluxes for vapors are generally less pronounced than those seen for gases, because the potential maximum concentrations of vapors are lower than those of gases under typical environmental conditions.

The two vapor diffusion examples represent reasonable, albeit simplified, cases of interest in the analysis of gaseous transport in contaminated subsurface environments. Both of these examples involve air (saturated with water

vapor) and a given VOC. In each case, the VOC is diffusing away from a constant pressure source of VOC-saturated moist air at 20°C and 1 atmosphere, and the opposite end of the column is open to a constant pressure source of clean, moist air at 20°C and 1 atmosphere. For these examples, the effective diffusion coefficient is taken to be 0.01 cm^2/sec. This value is based on a gas-filled porosity of 0.2, a tortuosity factor of 0.6, and a free-space diffusion coefficient of 0.083 for the VOC-air system.

The assumption here of isobaric conditions in the vicinity of a source of VOC vapors is not necessarily representative of typical field conditions. The typical source of subsurface VOC vapors is a liquid-phase solvent or nonaqueous phase liquid (NAPL). In homogeneous porous media, the evaporation of VOCs from a NAPL source would be expected to create a gas-phase pressure gradient, supporting viscous (Darcy) flux away from the NAPL. In the following two examples, the typically expected pressure gradient and advection caused by vaporization is neglected. In addition, VOC transfer to the gas phase is accompanied by local cooling due to the heat of vaporization, which is neglected here.

Figures 4-2 and 4-4 show the distributions of 1,1-dichloroethylene (1,1-DCE) and chloroform (TCM), respectively, predicted by the Graham Model for isobaric, isothermal countercurrent diffusion with moist air in open-ended horizontal porous media columns. These distributions

were calculated from the following analytical solution to equation (3-58) for steady-state conditions with no reactions or phase transfer

$$\chi_A = \frac{\{b\chi_A(0) + 1\}\left[\frac{b\chi_A(L) + 1}{b\chi_A(0) + 1}\right]^{(x/L)} - 1}{b} \qquad (4\text{-}7a)$$

where $b = \left[\frac{M_A}{M_B}\right]^{\frac{1}{2}} - 1$, x is the coordinate distance along a column of length L, $\chi_A(0)$ is the species A mole fraction at $x = 0$, and $\chi_A(L)$ is the species A mole fraction at $x = L$.

The analytical solution for the species A mole fraction distribution given by the Mass Model is identical in form to the solution for the Graham Model (equation (4-7a)), except that $b = \frac{M_A}{M_B} - 1$. With this alternative b factor, the Mass-Model equivalent to equation (4-7a) will be referred to here as equation (4-7b).

The Mole Model predicts a simple linear distribution of species mole fraction under steady, isobaric conditions

$$\chi_A = \left(\frac{\chi_A(L) - \chi_A(0)}{L}\right) x + \chi_A(0) \qquad (4\text{-}8)$$

For the distributions shown in Figures 4-2 through 4-5, the VOC (species A) mole fraction is taken as zero at $x = 0$. The VOC mole fraction at $x = L$ is at saturation for 20° C and 1 atmosphere (Boublik *et al.*, 1973). For reference, the molecular masses for 1,1-DCE, TCM, and moist air are taken to be 96.94, 119.4, and 28.7, respectively, in these examples.

As given by the Graham Model solution (equation (4-7a)) for isobaric countercurrent diffusion of 1,1-DCE and moist air, the mole fraction of 1,1-DCE varies as shown in Figure 4-2, along the 50 cm column from zero at the left end to 0.6547 at the right. The mole fraction distributions given by the Mass and Mole Model solutions (equations (4-7b) and (4-8), respectively) differ from that given by the Graham Model, as shown in Figure 4-3. Calculating diffusion fluxes using the mole-fraction derivatives given by each of the models gives the 1,1-DCE fluxes shown on Table 4-2.

An analogous case involving a less volatile chemical, chloroform, instead of 1,1-DCE, shows less difference between the steady-state diffusion fluxes predicted by the three models. The distributions of chloroform mole fraction, mass fraction, and mass density shown on Figure 4-4 were derived using the Graham Model. The mole fraction distributions given by all three models are shown on Figure 4-5. For countercurrent diffusion of chloroform and moist air, where the mole fraction of chloroform varies along the 50 cm column from zero at the left end to 0.2081 at the right, the model-predicted TCM fluxes are shown on Table 4-2.

As a final example of the differences in model-predicted diffusion flux, consider the countercurrent diffusion of argon and helium. Figure 4-6 shows the distribution of argon during steady, isobaric countercurrent diffusion with helium, where pure helium exists at the left-

hand end of the column and pure argon exists at the right-hand end of the column. Figure 4-7 shows the differing distributions of argon predicted by the three models under these conditions. The free-space diffusion coefficient for argon and helium is 0.7204 cm^2/sec. With the same air-filled porosity and tortuosity as the previous examples, the steady argon diffusion fluxes predicted by the Graham, Mole, and Mass Models are shown on Table 4-2.

Table 4-2. Comparison of model-predicted diffusion fluxes for the heavier species in binary mixtures under steady, isobaric conditions

	1,1-DCE/air		TCM/air		Argon/Helium	
A-D model	[1]-N_{DCE}	[2]Error	[1]-N_{TCM}	[2]Error	[1]-N_{Ar}	[2]Error
Mole Model	5.45	25.5%	1.73	10.5%	71.5	87.7%
Graham Model	4.34	0.0%	1.57	0.0%	38.1	0.0%
Mass Model	3.28	-24.4%	1.33	-15.1%	18.3	-51.9%

[1]Species flux units of (moles/cm^2s x 10^9)
[2]Relative percent difference of absolute flux values *versus* the Graham-Model flux

Because both the Graham and Mass Models predict that the molar fluxes of the lighter species in binary gas mixtures are significantly larger than those of the heavier species, the relative percent differences between model-predicted fluxes are larger for the lighter species, as shown in Table 4-3.

Table 4-3. Comparison of model-predicted diffusion fluxes for the lighter species in binary mixtures under steady, isobaric conditions

	1,1-DCE/air		TCM/air		Argon/Helium	
A-D model	[1]N_{air}	[2]Error	[1]N_{air}	[2]Error	[1]N_{He}	[2]Error
Mole Model	5.45	-31.7%	1.73	-45.9%	71.5	-40.6%
Graham Model	7.98	0.0%	3.20	0.0%	120.	0.0%
Mass Model	11.1	39.0%	5.53	73.1%	183.	51.9%

[1]Species flux units of (moles/cm^{2}s x 10^9)
[2]Relative percent difference of flux values *vs*. Graham Model

As a final comparison of the steady transport behavior predicted by the three A-D models, the total fluxes (sum of diffusive fluxes) predicted by the models under isobaric conditions are examined. For the same boundary conditions used to compute the species fluxes for Tables 4-2 and 4-3, the total molar fluxes predicted by the three A-D models are shown on Table 4-4.

Table 4-4. Comparison of model-predicted total molar fluxes under steady, isobaric conditions

	1,1-DCE/air		TCM/air		Argon/Helium	
A-D model	[1]N	[2]Error	[1]N	[2]Error	[1]N	[2]Error
Mole Model	0.0	-100%	0.0	-100%	0.0	-100%
Graham Model	3.64	0.0%	1.63	0.0%	82.3	0.0%
Mass Model	7.81	115%	4.20	158%	165.	100%

[1]Total molar flux units of (moles/cm^{2}s x 10^9)
[2]Relative percent difference in total flux *vs*. Graham Model

In the three example problems just presented, significant differences exist in the model-predicted steady-state diffusive fluxes. The largest differences in predicted flux occur between the Mass and Mole Models, with the flux predictions of the Graham Model falling in between the predictions of two traditional models. Based on the results from these three example problems, it appears that no general conclusions can be made regarding whether the Mass Model or the Mole Model better approximates the true VOC flux, as given by the Graham Model. In general, the traditional A-D transport models fail to represent significant processes that occur during gaseous countercurrrent diffusion.

To conclude this section on steady-state fluxes, the expected transport behavior under nonisobaric conditions is briefly discussed. The presence of a pressure gradient results in a viscous bulk flux, as described by Darcy's law, and the mole-fraction distribution is altered from the isobaric case. For the case of one-dimensional, axial equimolar countercurrent transport in a horizontal column, the Graham Model predicts that the mole fraction gradient is constant (i.e., the mole fraction curve is linear for the equimolar analogues of Figures 4-2, 4-4, and 4-6). The viscous flux is added to the nonequimolar flux to find the total molar flux, which becomes dominated by viscous flux under large pressure gradients.

Discussion of Transient Behavior

Comparing the transient behavior predicted by the models is important because certain effects occur under transient conditions that are not accounted for by comparing steady-state fluxes. Simulation of transient process behavior requires the use of the complete model formulations, where the diffusion equations and Darcy's law are incorporated into general continuity equations (e.g., equations (3-58) through (3-60)) and the required state equations (e.g., the ideal gas law) are utilized to close the resulting system of equations. Also, the Graham Model generally needs to be incorporated into a multiphase transport model to achieve reliable predictions of transport behavior. The non-linear nature of the transport models makes for difficult transient solutions, which will not be provided here. In lieu of solving the transport models for transient cases, the following qualitative discussion is offered to provide some insight into the nature of transient gaseous transport processes in porous media.

Recalling the process descriptions given in Chapter 2, a diffusion-induced pressure gradient will develop during countercurrent diffusion of species with differing molecular masses unless the system is completely open (e.g., a thin, highly permeable slab of porous medium bounded on both sides by regulated constant-pressure chambers). This type of behavior is well represented by the Graham Model. Such diffusion-induced pressure gradients are also predicted

using the Mass Model. However, the diffusion-induced pressure gradient predicted by the Mass Model for a closed column with boundary conditions of $\chi_{A1} = 1$ and $\chi_{A2} = 0$ at the column ends is twice that predicted by the Graham Model (Kramers and Kistemaker, 1943).

Other than Kramers and Kistemaker (1943), this predicted behavior has not been assessed previously using the Mass Model. This may be due to the fact that in prominently published works, the gas-phase has been taken as static and the gaseous equation of motion has not been explicitly solved (e.g., Abriola and Pinder, 1985b; Pinder and Abriola, 1986; Baehr and Corapcioglu, 1987). More recently developed numerical simulators have the capability to model a mobile gas phase, although the publications describing the use of these simulators have not mentioned the diffusion-induced pressure gradients that the Mass Model predicts.

In the transport model widely used in chemical engineering (the Mole Model), where equimolar diffusion is predicted under isobaric conditions, no diffusion-induced pressure gradients develop during countercurrent diffusion of species with differing molecular masses. Although this is also incorrect, as shown by Graham's law of diffusion, the Mole Model's lack of process fidelity does allow for simpler mathematical solutions.

To gain further insight into the nature of transient gaseous transport in porous media, consider the classic

diffusion problem involving a step change in gas composition (say for example to $\chi_A = 1$ at $t = 0$) at the vertical boundary of a semi-infinite medium with initial conditions of $\chi_A = 0$ and $P = 1$ atm. For a binary gas mixture with species of differing molecular mass, the Graham Model predicts the development of a pressure gradient and a corresponding viscous flux, so this classic "diffusion" problem can no longer be solved using the simple "diffusion equation" (Fick's second law of diffusion):

$$\frac{\partial}{\partial t}(C_A\theta_g) = D_{AB}^{*}\nabla^2 C_A \qquad (4\text{-}9)$$

As mentioned above, a rigorous analysis of this problem requires the solution of a non-linear A-D equation (equation (3-58), which will not be done here.

Nevertheless, based on the discussions and analyses presented in this dissertation, we know that if $M_A > M_B$, the diffusive molar flux of species *B* from the medium outward to the boundary will exceed the diffusive molar flux of species *A* into the medium from the boundary, and a vacuum ($P < 1$ atm) will be created in the medium. As indicated by inspection of the Graham Model continuity equation for the gas phase (equation (3-60)), the initially steep pressure gradient will decrease over time as the gradients in gas composition decrease. Although a quantitative solution to this problem will not be presented here, it can be concluded that the Graham-Model predicted species *A* flux from the boundary into the medium would be greater than that expected

in the absence of the diffusion-induced pressure gradient (as would be predicted by the Mole Model). If $M_A < M_B$, the diffusion-induced pressure gradient would be directed from the medium outward to the boundary, and the species A flux would be less than that expected under isobaric conditions.

A closely related problem of interest involves horizontal countercurrent transport in an infinite medium formed at time zero by joining two semi-infinite media along a common vertical boundary. An experimental analogue to this problem might consist of a long horizontal column of porous media, separated into two halves by a thin metal sheet. Say that the initial conditions for a binary gas system are $\chi_A = 1$ and $P = 1$ atm in the left half, and $\chi_A = 0$ and $P = 1$ atm in the right half. At time zero, the metal sheet is removed and countercurrent transport begins.

For $M_A > M_B$, the net diffusive molar flux, or nonequimolar flux, would be toward the left, producing a viscous flux toward the right. As discussed previously, these countercurrent bulk fluid fluxes would be of equal magnitude in a closed system, but the continuity requirements in an infinite medium are more complex. It seems reasonable to speculate that the magnitude of the molar species flux ratio at the "center" (joining plane) of the infinite medium would lie between the equimolar flux ratio found in a closed system and the Graham's law flux ratio found in a completely open, isobaric system (i.e., a very thin slab bounded on both sides by constant pressure).

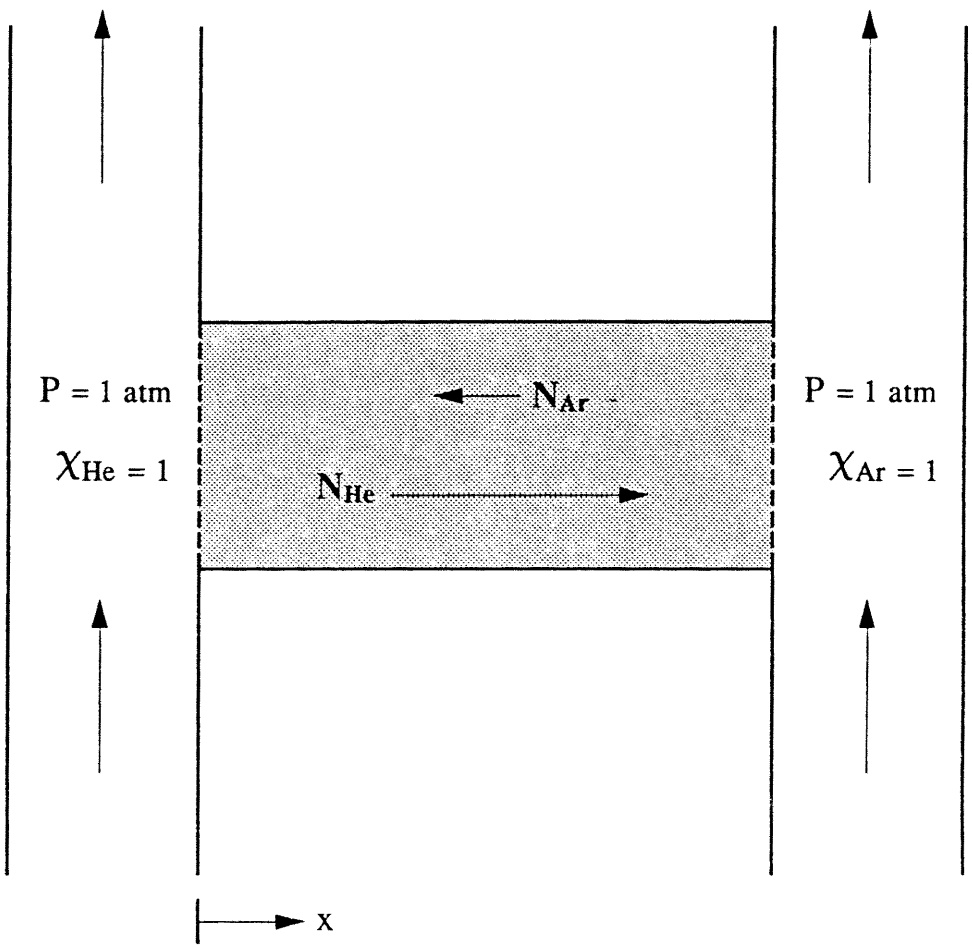

Figure 4-1. Isobaric countercurrent diffusion of helium and argon in an open-ended column of porous media.

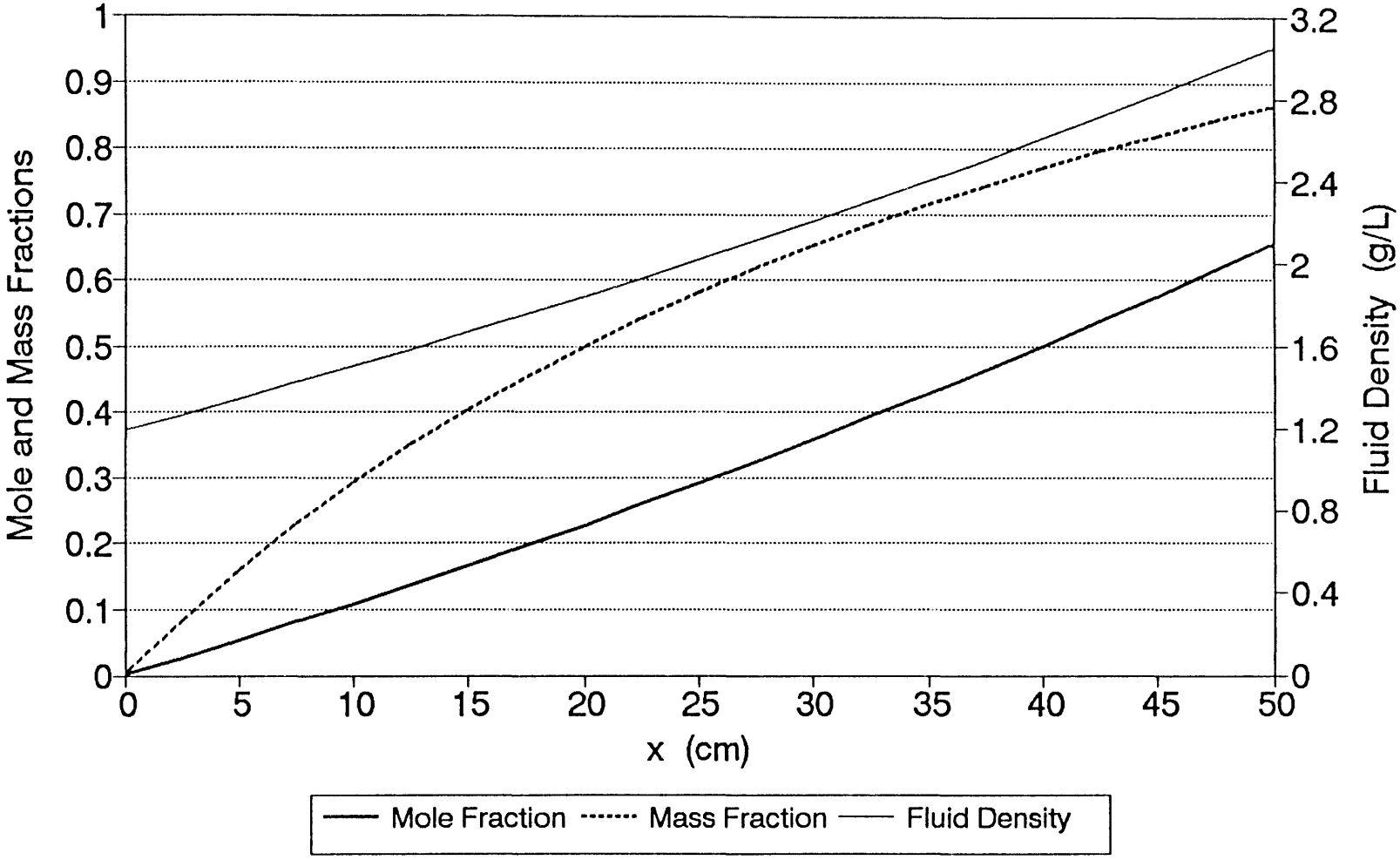

Figure 4-2. Steady-state 1,1-DCE distribution from Graham Model under isobaric conditions

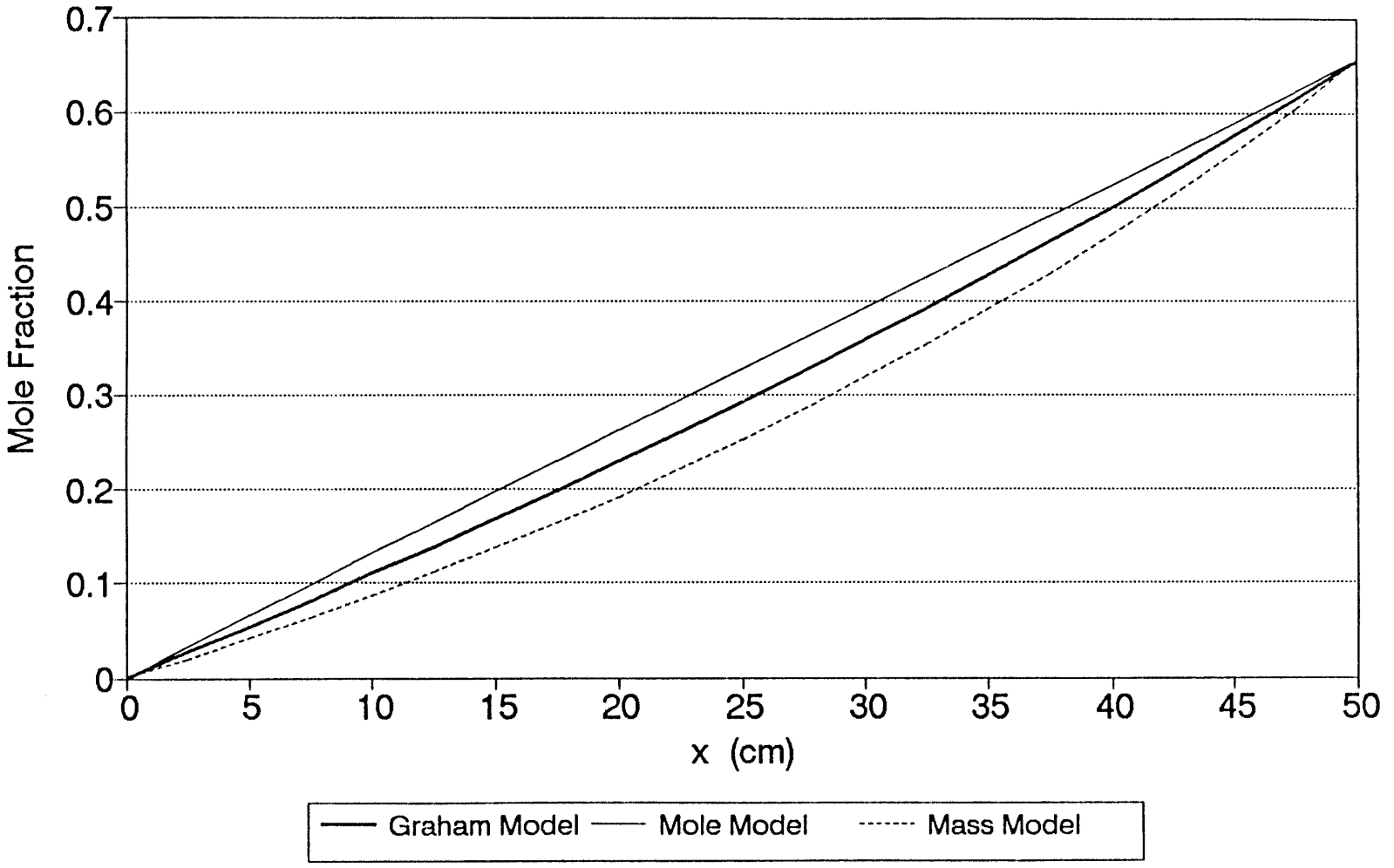

Figure 4-3. Steady model-predicted 1,1-DCE distributions under isobaric conditions

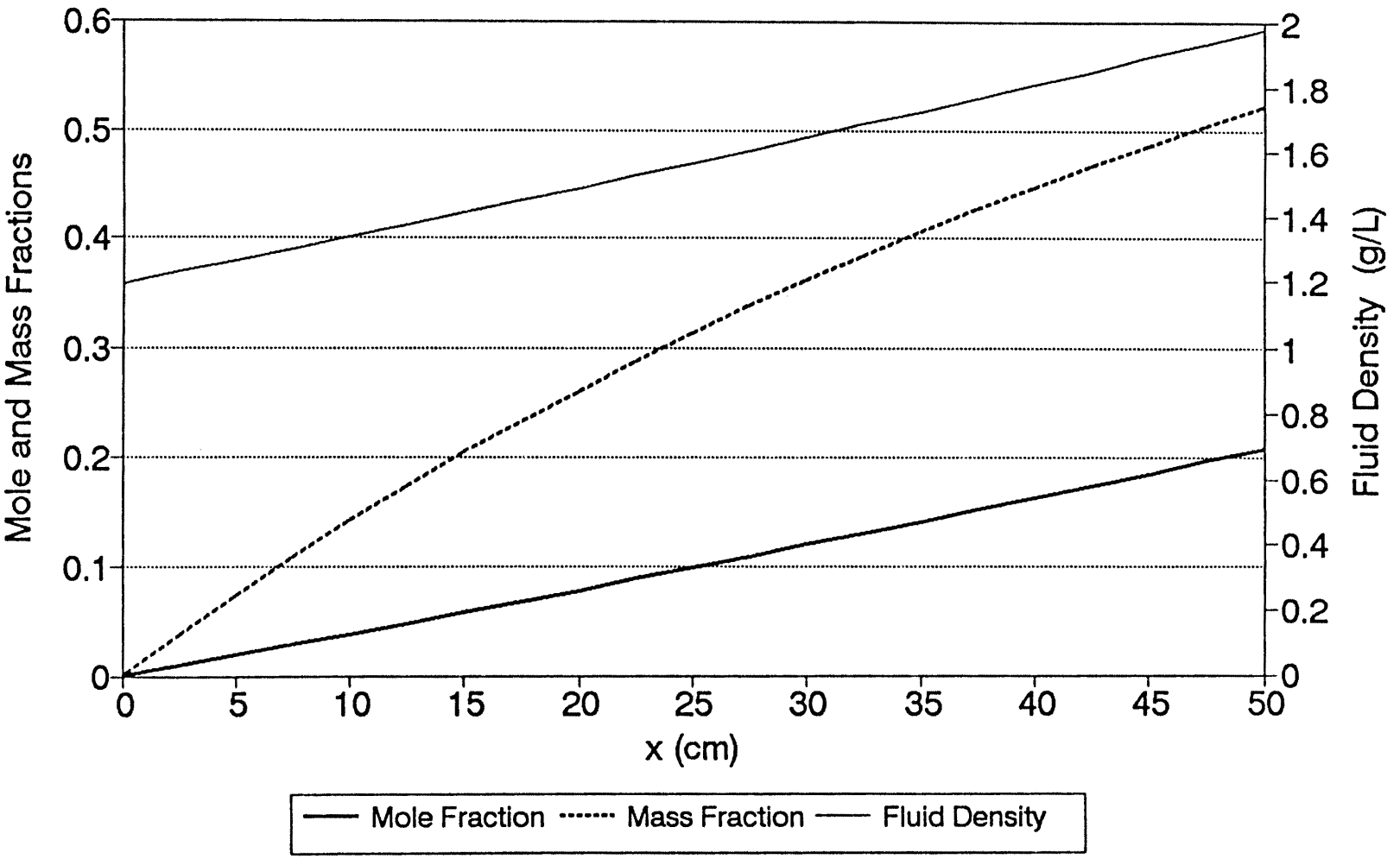

Figure 4-4. Steady-state chloroform distribution from Graham Model under isobaric conditions

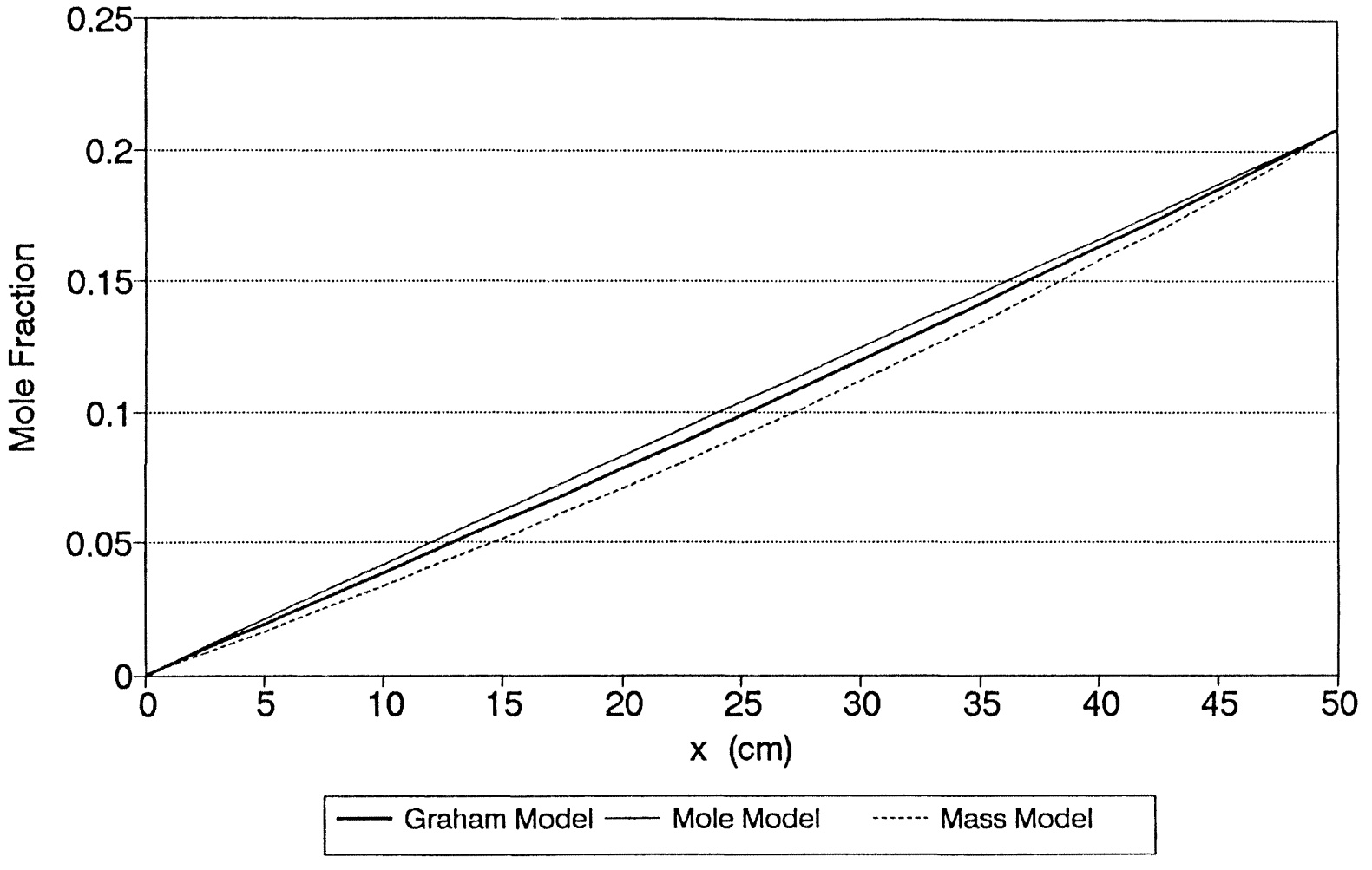

Figure 4-5. Steady model-predicted chloroform distributions under isobaric conditions

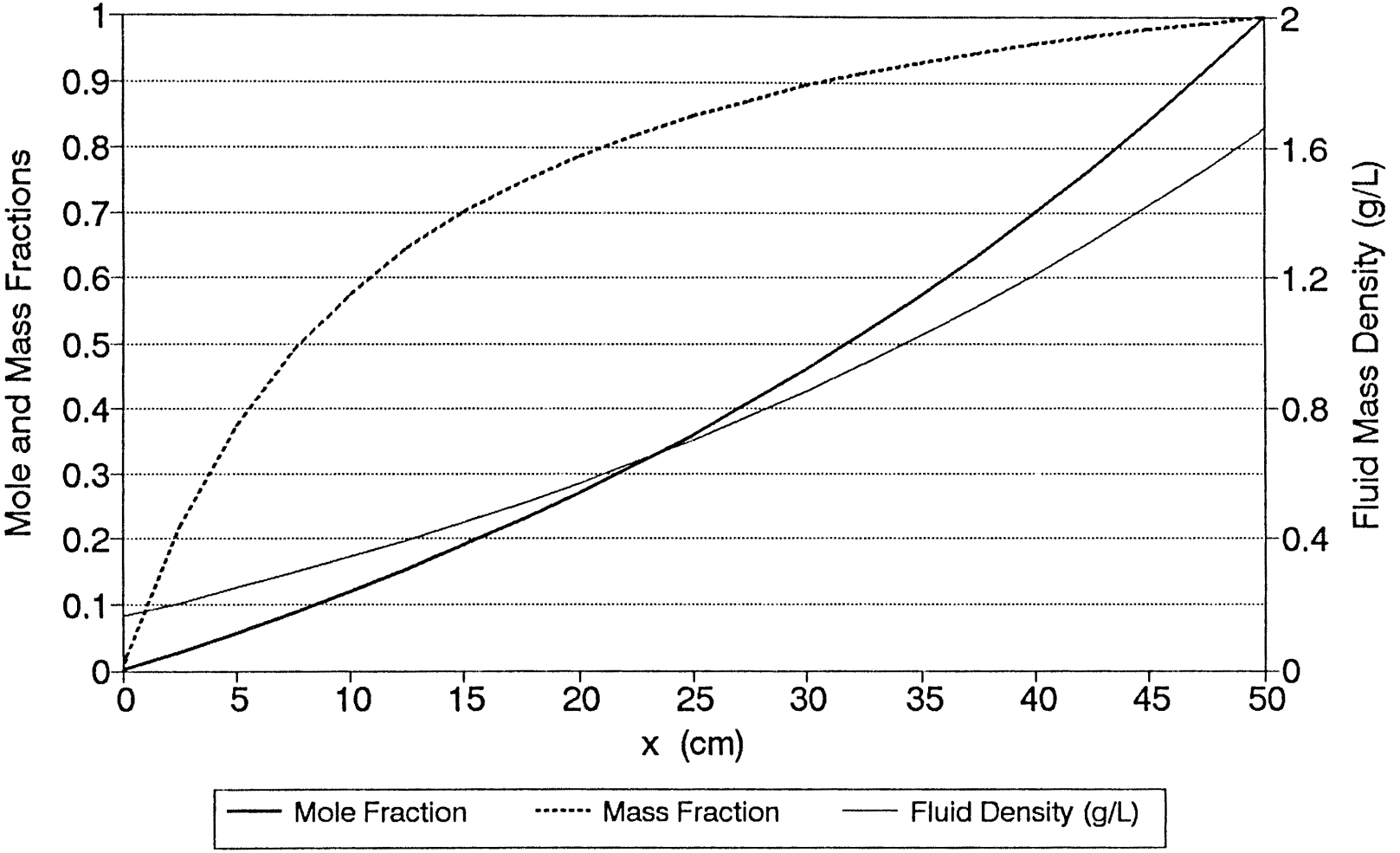

Figure 4-6. Steady-state argon distribution from Graham Model under isobaric conditions

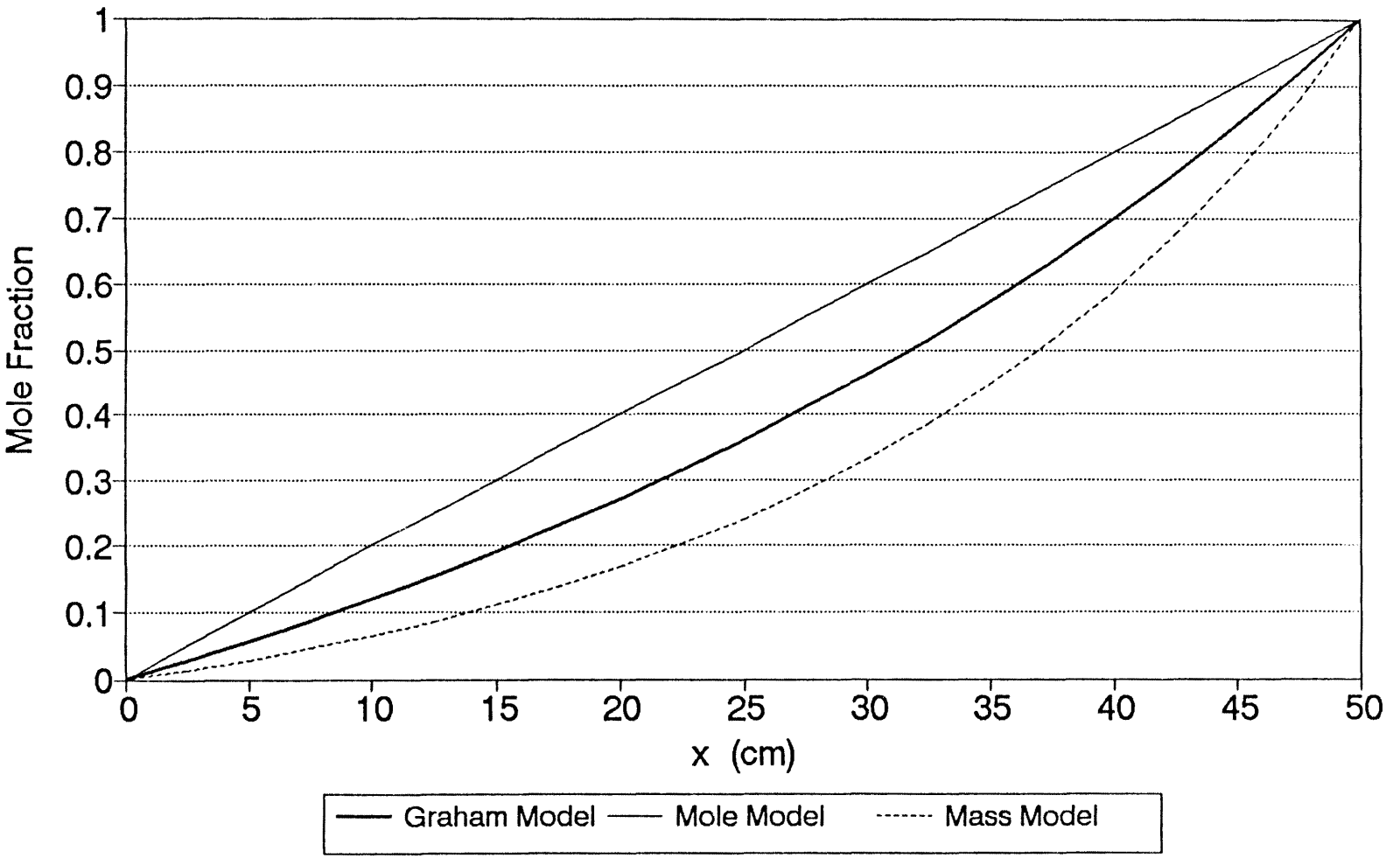

Figure 4-7. Steady model-predicted argon distributions under isobaric conditions

CHAPTER 5

MODEL COMPARISONS TO EXPERIMENTAL DATA

In this chapter, the capability of the three mathematical models to represent countercurrent transport of argon and helium in porous graphite will be examined by direct comparison with the experimental data of Evans, Truitt, and Watson (1961a, hereafter referred to as ET&W). It is shown that the Graham Model compares favorably with ET&W's data, and that neither the Mole Model nor the Mass Model adequately represent the physical processes active during ET&W's experiments.

It appears from a thorough literature review that ET&W's data may be the only "complete" set of data on transport of gases in porous media where the molecular diffusion regime prevails. (ET&W [1962a, 1963] also collected complete data sets for gaseous transport in very low-permeability porous media, although these data will not be discussed here due to the significant Knudsen/Klinkenberg effects seen in these data.) As mentioned in the literature review, the results of numerous countercurrent diffusion experiments have verified the fact that under isobaric, isothermal conditions, the ratio of binary species fluxes obeys Graham's law of diffusion precisely. However, other

than ET&W (1961a, 1962a, 1963), the experimenters have not generally collected all the data required to provide a true test of an A-D transport model. The majority of data reports have been presented in support of one or another of the multiple parameter transport models that appear in the literature. As might be expected, the curve-fits presented in these reports look impressive, but the lack of constraints imposed on parameter values and meanings leaves the predictive capability of these models in question. In order for an experimental data set to be considered "complete" for the purpose of testing the predictive capability of these models, there must be independent tests performed on the same porous medium to determine each independent parameter.

For the A-D transport models of interest here, there are three potentially adjustable parameters: permeability, porosity, and tortuosity. Thus, three independent types of experiments are required to determine the transport parameters. The intrinsic permeability should be measured according to standard methods using a pure fluid. If a gas is used in the measurement of permeability, several pressure levels should be used to determine the intrinsic permeability by the Klinkenberg approach. The diffusion experiments must include flux measurements for both species, along with measurements of pressure, temperature, and gradients of concentration and pressure. Pressure gradients must be measured with highly sensitive instruments due to

the fact that very small pressure gradients can produce significant gas flux. To test the predictive capability of a transport model, the parameter values obtained from such calibration experiments are used in the transport model to predict the results of independent experiments conducted on the same medium, preferably under different conditions.

The ET&W (1961a) data is particularly useful in testing the predictive capability of the Graham Model because the porous graphite used in ET&W's experiments had an intrinsic permeability of 2×10^{-10} cm^2. At near atmospheric pressure, this permeability is near the low-end limit where the molecular diffusion regime still prevails, but small Knudsen and Klinkenberg effects are detectable. Thus, ET&W's data provides a good indication of how the Graham Model performs near the lower limit of its applicability. In addition, the ratios of pressure gradient to viscous flux are larger in lower permeability media, making it easier to measure pressure gradients that may cause significant viscous flux.

For their experiments, ET&W used a thick-walled, hollow cylinder of porous graphite, with an axial length of 4 inches (10.16 cm), inside diameter of 0.5 inch (1.270 cm), and outside diameter of 0.8 inch (2.032 cm). The cylindrical porous medium was housed in a circulation chamber with provisions for controlling radial binary countercurrent flow and diffusion. Helium was circulated across the inner radial face and argon was circulated across the outer radial face of the porous medium to create steep

radial concentration gradients in the medium. The data from 22 experimental runs are presented by ET&W (1961a). Of the 22 experimental runs, 18 were conducted under almost isobaric conditions (what ET&W intended to be isobaric conditions), while the remaining 4 runs were conducted under a more significant applied pressure gradient.

ET&W present a pore-size distribution figure, along with porosity, specific surface, and adsorption data from independent measurements. The porous graphite had a bimodal pore-size spectrum with peak densities at the 0.2 and 2.5 micron pore radii, an interconnected porosity of 22%, and a specific surface of 0.64 m^2/g. The adsorption isotherms for both helium and argon indicate that surface diffusion was insignificant during ET&W's diffusion experiments. Pressure was measured by means of butyl phthalate manometers (fluid density = 1.046 g/cm^3), read to the nearest mm. This gave a pressure sensitivity of 0.0001 atm. Mass spectrometer analyses were used to determine argon and helium concentrations on both the inner and outer faces of the cylindrical porous medium.

ET&W did an excellent job of collecting, analyzing, and presenting their data. ET&W were among the early investigators who recognized the fact that Graham's law of diffusion correctly describes isobaric, isothermal diffusion of gases in porous media. Their experiments resulted in more complete data sets than previously available, enhanced

the understanding of governing processes, and provided a basis to develop better transport models (witness the DGM).

Because ET&W measured the fluxes of both gases, they could apply simple equations that account properly for the nonequimolar countercurrent diffusion. The equations used by ET&W are as follows:

$$\tilde{N} = \tilde{N}_A + \tilde{N}_B \tag{5-1}$$

$$\chi_A + \chi_B = 1 \tag{5-2}$$

$$D^*_{AB}\frac{d\chi_A}{dr} = -D^*_{BA}\frac{d\chi_B}{dr} \tag{5-3}$$

and

$$\tilde{N}_A = \chi_A\tilde{N} - A\frac{P}{RT}D^*_{AB}\frac{d\chi_A}{dr} \tag{5-4}$$

where $\tilde{N}_A$ is the species A molar transport rate (product of flux and area normal to the radial flux vector), $\tilde{N}$ is the total molar transport rate, b is the axial length of the cylindrical porous medium, and $A = 2\pi rb$.

Equation (5-4) can be integrated, using as boundary conditions the mole fractions of species A at the inner and outer radii of the porous medium (r_1 and r_2, respectively). This yields the expression used by ET&W to determine effective diffusion coefficients from their experimental results:

$$\tilde{N} = D_{AB}^{*}\left(\frac{A}{L}\right)^{*}\frac{P}{RT}\ln\left[\frac{\tilde{N}_A - \chi_A(r_2)\tilde{N}}{\tilde{N}_A - \chi_A(r_1)\tilde{N}}\right] \qquad (5\text{-}5)$$

where $(A/L)^{*} = (2\pi b)/ln(r_2/r_1)$. This expression yields essentially exact diffusion coefficients from the flux data, as shown in the right-hand column of Table 5-1. Although the equations used by ET&W are useful for the purpose of determining diffusion coefficients when both species fluxes are measured, they do not serve as a predictive transport model because there is no constitutive relation for predicting bulk advective fluxes.

It should be noted that although in ET&W's Tables I and II, they do not footnote the existence of a pressure gradient during the first 18 experimental runs (which were intended to be isobaric), they state in their text that "approximately 1 mm (of butyl phthalate) pressure difference was inadvertently maintained during all experiments". This translates to a pressure difference of 100 dynes/cm^2 across the porous medium. To explain the fact that ET&W's average observed flux ratio exceeded that given by Graham's law (i.e., 3.285 mean observed ratio versus 3.159 by Graham's law), the pressure must have been greater at the inner radius, where helium was circulated during ET&W's experiments. Apparently, ET&W thought that this pressure difference was too small to be of concern, but it will be shown here that it is large enough to explain the fact that the observed molar flux ratios are larger than expected by Graham's law during isobaric countercurrent diffusion.

To account for viscous flux and more fully explain ET&W's data, the permeability data presented by ET&W was used to evaluate Darcy fluxes under the given pressure gradients. ET&W present a plot of 31 permeability measurements, made with helium and argon (separately) over a pressure range of 1/2 to 1/8 atmosphere. The permeability data for each gas extrapolated to an intrinsic permeability of 2.0×10^{-10} cm^2 at high pressure. The permeabilities measured with both gases increased with decreasing pressure (the Klinkenberg effect). Helium showed a more pronounced Klinkenberg effect, as expected, because the mean free path of helium is over 2 times as large as that of argon. Because ET&W's experiments were conducted at pressures of 1.25 to 6.35 atm, however, Klinkenberg and Knudsen effects on the data appear to be minimal.

In comparison to the diffusion coefficients calculated by ET&W, the model-fit diffusion coefficients shown in Table 5-1 were calculated in an approximate manner using the Graham model, as given by equation (3-52) for steady-state conditions with no reactions or phase transfer. Casting in terms of molar transport rates, and using a finite difference approximation for the mole-fraction gradient, equation (3-55) is re-arranged to give

$$D^*_{AB} = \phi\tau D_{AB} = \frac{\left[\chi_A \tilde{N}^V - \tilde{N}_A\right] f_{Xa} L}{c\, A\, \Delta\chi_a} \qquad (5\text{-}6)$$

where ϕ = porosity, τ = tortuosity, $A = 2\pi\bar{r}b$, $\bar{r} = (r_1+r_2)/2$, $L = r_2 - r_1$, $\Delta\chi_A = \chi_{A2} - \chi_{A1}$, and

$$f_{Xa} = \left\{ \left(\frac{M_A}{M_B} \right)^{\frac{1}{2}} - 1 \right\} \chi_A + 1 \qquad (5\text{-}7)$$

The f_{Xa} factor is simply a rearrangement of the inverse of the bracketed coefficient in equation (3-32). The horizontal molar flow rate is given by Darcy's law, using a finite difference approximation for the pressure gradient

$$\tilde{N}^V = \frac{-kP}{\mu RT} A \frac{\Delta P}{L} \qquad (5\text{-}8)$$

where $\Delta P = P_2 - P_1$. (For hydrologists accustomed to working with the volume flow rate form of Darcy's law, $\tilde{N}^V = (P/RT)Q = cQ$, where Q is the Darcy volume flow rate.)

The mole fraction of helium (species *A*) appearing in equation (5-6) was taken as the arithmetic mean of the boundary mole fractions. This mean mole fraction for helium, and that for argon were then used to estimate average mixture viscosities at temperatures of 298.5°K and 373.15°K, applicable to ET&W's experimental Runs 1 through 14, and 15 through 22, respectively. The mixture viscosities, estimated according to the method of Wilke (1950), are 236.0 micropoise at 298.5°K and 279.0 micropoise at 373.15°K. These viscosities were taken as representative for all *r*. In reality, the viscosity (at a given temperature) would vary by up to 15% as a function of the varying composition along the radial coordinate. The effects of this variation on the total species flux would be relatively small during ET&W's experiments, however, because

the viscous flux represented only a fraction of the total species flux.

During experimental Runs 1 through 18, viscous species fluxes varied from 0.3% to 9.3% of the total species fluxes, and during Runs 19 through 22, viscous species fluxes varied from 9.7% to 28.9% of the total species fluxes. Because the molar diffusive flux of argon was less than that of helium, and because the viscous fluxes of both argon and helium were nearly equivalent, the average ratio of viscous to total species flux was larger for argon than helium. For experimental Runs 1 through 18, the total viscous flux (Darcy molar flux, $\tilde{\mathbf{N}}^V$) averaged only 2.4% of the total molar flux ($\tilde{\mathbf{N}} = c\mathbf{v}^N$). It is noteworthy that while significant bulk flow occurred during these experiments, the viscous flux accounted for only a small fraction of the bulk flow. In Runs 19 through 22, with the larger pressure gradient, the total viscous flux averaged 33.1% of the total molar flux. Also, as expected, the ratio of viscous to total flux increases with increased pressure, due to increased total molar concentration, c (i.e., $\tilde{\mathbf{N}}^V = c\mathbf{Q}$).

The distributions of argon and helium during ET&W's countercurrent diffusion experiments can be approximated using an analytical solution to the Graham Model equation (3-58). Analogous to the solution used to obtain the steady-state distributions shown in Figures 4-2, 4-4, and 4-6, equation (3-58) can be solved for the steady radial distribution (in cylindrical coordinates) of helium under

isobaric conditions. Assuming that pure helium exists at the inner radius ($\chi_A = 1$ at $r = r_1$) and pure argon exists at the outer radius ($\chi_A = 0$ at $r = r_2$), the distribution of helium is given by

$$\chi_A = \frac{\exp\left[\ln\left(\frac{M_A}{M_B}\right)^{\frac{1}{2}} \frac{\ln(r_2/r)}{\ln(r_2/r_1)}\right] - 1}{\left[\frac{M_A}{M_B}\right]^{\frac{1}{2}} - 1} \qquad (5\text{-}9)$$

Equation (5-9) was used to obtain the helium distribution shown on Figure 5-1. The boundary conditions used to derive equation (5-9) and the helium distribution shown in Figure 5-1 are similar to those in effect during Runs 1-18 of ET&W's experiments. During ET&W's experiments, however, the average mole fractions of helium at the inner and outer porous medium radii were actually 0.9871 and 0.0381, respectively, and small pressure gradients also existed. The pressure difference ($P_2 - P_1$) across the porous medium was approximately -100 dynes/cm^2 during experimental Runs 1 through 18, and 1800 dynes/cm^2 during Runs 19 through 22. The presence of a pressure gradient alters the mole-fraction distribution. For ET&W's experiments, positive pressure differences (such as existed during experimental Runs 19 through 22) flatten out the helium mole-fraction distribution curve to a point (see Chapter 4), whereas negative pressure gradients accentuate the curvature of the mole-fraction curve.

Figure 5-1, which roughly approximates the average helium distribution during ET&W's experiments, indicates that the mole fraction of helium at the mean porous medium radius is expected to deviate slightly from the arithmetic mean of boundary mole fractions used to evaluate χ_A in equation (5-6). Approximation errors in the mean mole fraction used in fitting equation (5-6) to ET&W's data affect the estimates of the effective diffusion coefficient and the tortuosity (i.e., the estimates deviate from the "actual tortuosity"). However, because the graphite porosity and permeability were measured independently, tortuosity is the only adjustable calibration parameter. Thus, a good fit of the model using only one adjustable parameter lends support to the model's predictive capability.

For the comparisons of the Mole and Mass Models to ET&W's data, the same general method as described above was used. Equations analogous to equation (5-6) were used, with alternate definitions of the f_{Xa} factor. For the Mole Model, $f_{Xa} = 1$, and for the Mass Model

$$f_{Xa} = \left\{ \left(\frac{M_A}{M_B} \right) - 1 \right\} \chi_A + 1 \qquad (5\text{-}10)$$

It should be emphasized that the general method used to compare all three transport models to ET&W's data is approximate due to the finite difference approximations in the gradients of mole fraction and pressure, and the estimated mole fractions and pressures at the mean radius of

the porous medium. The specific approximations involved with the simplified method of analysis are:

1. The mole-fraction gradient is approximated using only the boundary mole fractions. This gradient approximation can be viewed as consisting of two elements. The first is simply the finite-difference approximation error in estimating the point gradient at the mean radius of the cylindrical porous medium. For the isobaric case, the error associated with this finite-difference approximation (using the Graham Model) can be roughly assessed by examination of Figure 5-1. Differential boundary pressures will alter the species mole-fraction distribution in qualitatively predictable ways, as previously mentioned. The second, more complex element of the mole-fraction gradient approximation derives from the fact that the model-predicted species mole-fraction distributions (for specified boundary conditions) differ for each transport model (as shown in Figures 4-3, 4-5, and 4-7). Thus, the gradient approximation errors differ for each model.
2. The gas composition at the mean radius of the porous medium is estimated as the mean of boundary mole fractions. For the Graham Model, the error associated with this approximation can be roughly estimated by examination of Figure 5-1, realizing that differential

boundary pressures will alter the mole-fraction distribution. For the isobaric case shown in Figure 5-1, it appears that the error in mole-fraction estimates would be on the order of 14%.

3. The pressure gradient is approximated using only the boundary pressures. This gradient approximation also involves two elements. To estimate the errors associated with the pressure gradient approximation requires the model-predicted radial pressure distributions for each model (say for average experimental boundary conditions). The predicted pressure distributions (for specified boundary conditions) differ for each model, and thus the gradient approximation errors differ for each model. Because the pressure gradients were very small during ET&W's experiments, the errors associated with this particular approximation are considered negligible.

4. The gas pressure at the mean radius of the porous medium is estimated as the mean of boundary pressures. The approximation error associated with this estimate is analogous to that described above for the estimated mole fraction at the mean radius of the porous medium, except that the pressure gradients that existed were very small compared to the mole-fraction gradients. Thus, the errors associated with this particular approximation are also considered negligible.

Comparison of Graham Model to Experimental Data

The results of the Graham Model fit to ET&W's data are shown on Table 5-1. For each experimental run, an effective diffusion coefficient was determined using equation (5-6). The 22 model-fitted effective diffusion coefficients were then averaged, and the mean effective diffusion coefficient was used, along with the independent porosity measure (22%), to determine an estimated tortuosity of 0.0421. This single estimate of tortuosity was then used in the steady-state versions of equations (3-58) and (3-59), assuming no reactions and no phase transfer, to predict the species transport rates for all 22 experimental runs. The predicted species transport rates for each run were then added to obtain the total transport rates, and ratios of the species transport rates were formed to obtain the model-predicted values shown on Table 5-1. Although this was done using the helium flux data for the presentation on Table 5-1, this can also be done using either the argon flux data or the total molar flux data.

Using the helium, argon, and total flux data resulted in estimated mean effective diffusion coefficients of 0.00667 cm^2/sec, 0.00664 cm^2/sec, and 0.00668 cm^2/sec, respectively. The standard deviations of the estimated diffusion coefficients (with n-1 weighting, for all 22 experimental runs) are 0.000286, 0.000445, 0.000381, respectively. Using pooled estimates of variance, the mean model-predicted transport rates and flux ratios all test

statistically (at > 99% confidence) to be equivalent to the mean experimentally observed transport rates and flux ratios.

The model-predicted transport rates also compare well over the range of observed transport rates for the individual experimental runs, in which temperature, pressure, and pressure gradient all varied significantly. Thus, the steady-state version of the Graham Model (with two terms and two parameters) demonstrates its versatility in accounting for viscous, nonequimolar, and molecular diffusion fluxes under the varied conditions of ET&W's experiments.

It is noteworthy that the tortuosity estimated from ET&W's data is significantly lower than that given by the Millington (1959) equation. Although there is some evidence that the Millington equation works well for soils (for which it was developed), it does not work well for the porous graphite used by ET&W. Porous graphite varies greatly in structure, depending on how it is processed, and the tortuosity varies accordingly. Thus, without knowing the details of how ET&W's graphite was processed, it is fruitless to speculate about whether the tortuosity is unreasonably low or not. For reference purposes, Cunningham and Williams (1980) cite a typical tortuosity range of 0.143 to 0.333, which is supported by over 600 experimental results on 23 porous catalysts. The lowest tortuosity shown in Cunningham and Williams' data summary is 0.0287, which

was determined based on 12 experimental results for the same medium.

To provide a test of the Graham Model's capability in predicting viscous and diffusive fluxes, ET&W's data is divided into two groups: the (almost) isobaric experimental Runs 1-18, and the differential pressure Runs 19-22. The effective diffusion coefficient in the Graham Model is fitted to the data from Runs 1-18 (Table 5-2), as was done previously using all 22 runs, and the fluxes and flux ratios for Runs 19-22 are predicted (Table 5-3). The effective diffusion coefficients shown on Table 5-2 are fitted to the helium flux data, although the argon flux data and the total flux data both yield almost identical diffusion coefficients. The mean effective diffusion coefficients for Runs 1-18 using the helium, argon, and total flux data are 0.00674 cm^2/sec, 0.00673 cm^2/sec, and 0.00674 cm^2/sec, respectively, resulting in an tortuosity estimate of 0.0425.

Using the mean effective diffusion coefficient of 0.00674 cm^2/sec, permeability of 2×10^{-10} cm^2, temperature of 373.2°K, differential pressure of 1800 $dynes/cm^2$, and the mean pressures and boundary mole fractions for Runs 19-22, the calibrated Graham Model predicts the fluxes and flux ratios shown on Table 5-3. Although the predicted species fluxes appear to show a slight bias on the high side (reflecting the high bias in the estimated effective diffusion coefficient), the model-predicted flux ratios agree very well with ET&W's data for Runs 19-22.

Comparisons of the Mole and Mass Models to Experimental Data

As will be shown here, neither the Mole Model nor the Mass Model, as given by equations (3-56) and (3-57), respectively, adequately represent ET&W's experimental data.

Ignoring for the moment the small pressure gradients that existed during ET&W's experiments, the Mole Model predicts equimolar countercurrent fluxes if a single effective diffusion coefficient is used for both the helium and argon flux predictions (see Chapter 4). Likewise, the Mass Model predicts equimass countercurrent fluxes if a single effective diffusion coefficient (or tortuosity) is used for both the argon and helium flux predictions. Thus, for the case of argon and helium, the predicted ratios of species molar fluxes given by the Mole and Mass Models are -1.00 and -9.98, respectively, as compared to the Graham Model's predicted flux ratio of -3.16. Accounting for the viscous flux due to the pressure gradients that existed during ET&W's experimental Runs 1-18 alters the Mole and Mass Model predictions only slightly, as the viscous flux accounting in the Graham Model predictions did (i.e., the average Graham-Model predicted flux ratio changed from 3.16 for isobaric to 3.28 under the pressure gradients of Runs 1-18).

Because the Mole Model does not account for the non-equimolar flux, it fails dramatically in cases such as the experiments of ET&W, where the nonequimolar flux dominates. The Mole Model predicts an average total molar flux of only

about 2.4% of the measured flux for ET&W's Runs 1-18, when a small negative pressure gradient existed. For Runs 19-22, when a significant positive pressure gradient existed, the Mole Model predicts a negative total molar flux, according to Darcy's law. The measured total molar flux for Runs 19-22 is actually in the positive r direction, as shown on Table 5-1, because the nonequimolar flux dominates over the viscous flux. Because the Mass Model significantly over predicts the nonequimolar flux, it can also produce errors in the sign of predicted total molar flux.

Thus, both the Mole and Mass Models fail to adequately describe steady-state gas transport in cases where the fluid density varies significantly with fluid composition. The Mole and Mass Models can be made to represent data such as ET&W's by using different effective diffusion coefficients (or tortuosities) to model each species flux. However, when this is done, the meaning of the tortuosity parameter (as a property of the porous medium alone) is lost, and the resulting "tortuosities" are dependent on fluid composition. This makes the models more difficult to calibrate and use for predictive purposes.

The average effective diffusion coefficients resulting from fitting the Mole Model to ET&W's data are

$$D_{AB}^{*} = 0.0103$$

and

$$D^{*}_{BA} = 0.00324$$

The corresponding species-specific tortuosities are

$$\tau^{N}_{A} = 0.0648$$

and

$$\tau^{N}_{B} = 0.0204$$

which are significantly different. Similarly, the effective diffusion coefficients resulting from fitting the Mass Model to ET&W's data are

$$D^{*}_{AB} = 0.00553$$

and

$$D^{*}_{BA} = 0.0174$$

The corresponding species-specific tortuosities are

$$\tau^{M}_{A} = 0.0349$$

and

$$\tau^{M}_{B} = 0.110.$$

Table 5-1. Graham Model fit to measured transport rates of Evans, *et al.* (1961a)

Exper. Run No.[1,2]	Temp (°K)	Pressure (atm)	Mole fraction of helium		Transport rates (moles/sec x 10^5)						Ratio $-(\bar{N}_{He}/\bar{N}_{Ar})$		Effective diffusion coeff.[4], D_{AB}^*, (cm^2/sec x 10^3)	
					$\bar{N}_{He}$		$-\bar{N}_{Ar}$		$\bar{N}$					
			at $r=r_1$	at $r=r_2$	Model	Meas.	Model	Meas.	Model	Meas.	Model	Meas.	Model	ET&W[5]
1	299.7	1.249	.9935	.0232	5.83	6.07	1.81	1.72	4.02	4.35	3.23	3.53	6.95	6.17
2	298.4	1.251	.9866	.0446	5.68	5.75	1.76	1.73	3.92	4.02	3.23	3.32	6.75	6.17
3	297.1	1.251	.9867	.0439	5.67	5.66	1.76	1.71	3.91	3.94	3.23	3.31	6.66	6.11
4	301.1	1.475	.9874	.0454	5.73	5.78	1.77	1.61	3.96	4.17	3.24	3.59	6.73	5.97
5	299.3	1.475	.9862	.0434	5.70	5.52	1.76	1.77	3.94	3.75	3.24	3.12	6.46	6.06
6	300.5	1.500	.9947	.0169	5.87	6.18	1.81	1.94	4.06	4.24	3.24	3.19	7.02	6.49
7	298.7	1.740	.9962	.0132	5.88	6.14	1.81	1.80	4.07	4.34	3.25	3.41	6.97	6.27
8	295.7	1.740	.9863	.0419	5.66	5.45	1.74	1.79	3.92	3.66	3.26	3.04	6.42	6.09
9	295.4	1.975	.9862	.0440	5.66	5.69	1.73	1.80	3.93	3.90	3.27	3.16	6.71	6.27
10	297.3	1.992	.9958	.0132	5.86	6.03	1.79	1.92	4.07	4.11	3.27	3.14	6.86	6.40
11	298.7	3.005	.9872	.0442	5.74	5.79	1.72	1.70	4.01	4.09	3.33	3.41	6.73	6.14
12	300.5	3.005	.9861	.0421	5.76	5.49	1.73	1.84	4.03	3.64	3.33	2.98	6.35	6.13
13	298.1	3.704	.9950	.0146	5.90	6.18	1.75	2.13	4.15	4.05	3.37	2.90	6.99	6.77
14	298.2	6.351	.9857	.0358	5.82	6.35	1.65	1.64	4.18	4.71	3.54	3.87	7.29	6.40
15	373.2	1.25	.9851	.0485	6.67	6.30	2.09	1.95	4.59	4.35	3.20	3.23	6.29	5.81
16	373.2	1.48	.9846	.0507	6.67	6.50	2.08	2.00	4.59	4.51	3.21	3.25	6.50	6.00
17	373.2	1.96	.9844	.0508	6.67	6.63	2.07	2.02	4.60	4.61	3.22	3.29	6.63	6.10
18	373.2	2.51	.9842	.0532	6.67	6.93	2.06	2.05	4.61	4.88	3.24	3.39	6.93	6.31
19	373.2	1.98	.9834	.0375	6.09	5.89	2.68	2.51	3.41	3.38	2.27	2.34	6.47	6.17
20	373.2	1.51	.9789	.0489	6.13	5.78	2.51	2.36	3.62	3.42	2.44	2.45	6.31	6.04
21	373.2	1.27	.9829	.0423	6.27	5.77	2.47	2.30	3.81	3.47	2.54	2.51	6.16	5.90
22	373.2	2.97	.9783	.0397	5.73	5.59	2.94	2.90	2.79	2.69	1.95	1.93	6.53	6.44
Mean	325.6	2.120	.9871	.0381	5.984	5.976	1.976	1.963	4.009	4.013	3.272[3]	3.285[3]	6.668[6]	6.191

[1] For Runs 1-18, ΔP = -100 dynes/cm^2

[2] For Runs 19-22, ΔP = 1800 dynes/cm^2

[3] Flux ratio means are for Runs 1-18 only

[4] Normalized to 20° C and 1 atm by $D = D_0(P_0/P)(T/T_0)^{1.75}$, D_0 = 0.7204 cm^2/sec

[5] Evans, Truitt, and Watson's (1961a) model-fit diffusion coefficients

[6] D_{AB}^* = 6.67 x 10^{-3} cm^2/sec (arithmetic mean of 22 values) used for model-based transport rates

Table 5-2. Graham Model calibration using data from Runs 1-18 of Evans, *et al.* (1961a)

Exper. Run No.[1]	Temp (°K)	Pressure (atm)	Mole fraction of helium		Transport rates (moles/sec x 10^5)			Ratio $-(\bar{N}_{He}/\bar{N}_{Ar})$	Effective diffusion coeff.[2], D_{AB}^*, (cm^2/sec x 10^3)
					$\bar{N}_{He}$	$-\bar{N}_{Ar}$	$\bar{N}$		
			at $r = r_1$	at $r = r_2$	Meas.	Meas.	Meas.	Meas.	Model
1	299.7	1.249	.9935	.0232	6.07	1.72	4.35	3.53	6.95
2	298.4	1.251	.9866	.0446	5.75	1.73	4.02	3.32	6.75
3	297.1	1.251	.9867	.0439	5.66	1.71	3.94	3.31	6.66
4	301.1	1.475	.9874	.0454	5.78	1.61	4.17	3.59	6.73
5	299.3	1.475	.9862	.0434	5.52	1.77	3.75	3.12	6.46
6	300.5	1.500	.9947	.0169	6.18	1.94	4.24	3.19	7.02
7	298.7	1.740	.9962	.0132	6.14	1.80	4.34	3.41	6.97
8	295.7	1.740	.9863	.0419	5.45	1.79	3.66	3.04	6.42
9	295.4	1.975	.9862	.0440	5.69	1.80	3.90	3.16	6.71
10	297.3	1.992	.9958	.0132	6.03	1.92	4.11	3.14	6.86
11	298.7	3.005	.9872	.0442	5.79	1.70	4.09	3.41	6.73
12	300.5	3.005	.9861	.0421	5.49	1.84	3.64	2.98	6.35
13	298.1	3.704	.9950	.0146	6.18	2.13	4.05	2.90	6.99
14	298.2	6.351	.9857	.0358	6.35	1.64	4.71	3.87	7.29
15	373.2	1.25	.9851	.0485	6.30	1.95	4.35	3.23	6.29
16	373.2	1.48	.9846	.0507	6.50	2.0	4.51	3.25	6.50
17	373.2	1.96	.9844	.0508	6.63	2.02	4.61	3.29	6.63
18	373.2	2.51	.9842	.0532	6.93	2.05	4.88	3.39	6.93
Means	315.1	2.162	.9884	.0372	6.024	1.840	4.184	3.285	6.735[3]

[1] For Runs 1-18, ΔP = -100 dynes/cm^2

[2] Normalized to 20° C and 1 atm by $D = D_0(P_0/P)(T/T_0)^{1.75}$, D_0 = 0.7204 cm^2/sec

[3] D_{AB}^* = 6.74 x 10^{-3} cm^2/sec (arithmetic mean of 18 values) used for model predictions shown on Table 5-3

Table 5-3. Graham Model predictions for experimental Runs 19-22 of Evans, *et al.* (1961a)

Exper. Run No.[1]	Temp (°K)	Pressure (atm)	Mole fraction of helium		Transport rates[2] (moles/sec x 10^5)						Ratio $-(\hat{N}_{He}/\hat{N}_{Ar})$	
					$\hat{N}_{He}$		$-\hat{N}_{Ar}$		$\hat{N}$			
			at $r = r_1$	at $r = r_2$	Model	Meas.	Model	Meas.	Model	Meas.	Model	Meas.
19	373.2	1.98	.9834	.0375	6.16	5.89	2.70	2.51	3.46	3.38	2.28	2.34
20	373.2	1.51	.9789	.0489	6.20	5.78	2.53	2.36	3.67	3.42	2.45	2.45
21	373.2	1.27	.9829	.0423	6.34	5.77	2.49	2.30	3.86	3.47	2.55	2.51
22	373.2	2.97	.9783	.0397	5.80	5.59	2.97	2.90	2.84	2.69	1.96	1.93
Means	373.2	1.93	.9809	.0421	6.13	5.76	2.67	2.52	3.45	3.24	2.31	2.31[3]

[1] For Runs 19-22, ΔP = 1800 dynes/cm^2

[2] D_{AB}° = 6.74 x 10^{-3} cm^2/sec (arithmetic mean of 18 values from Table 5-2) used for model predictions

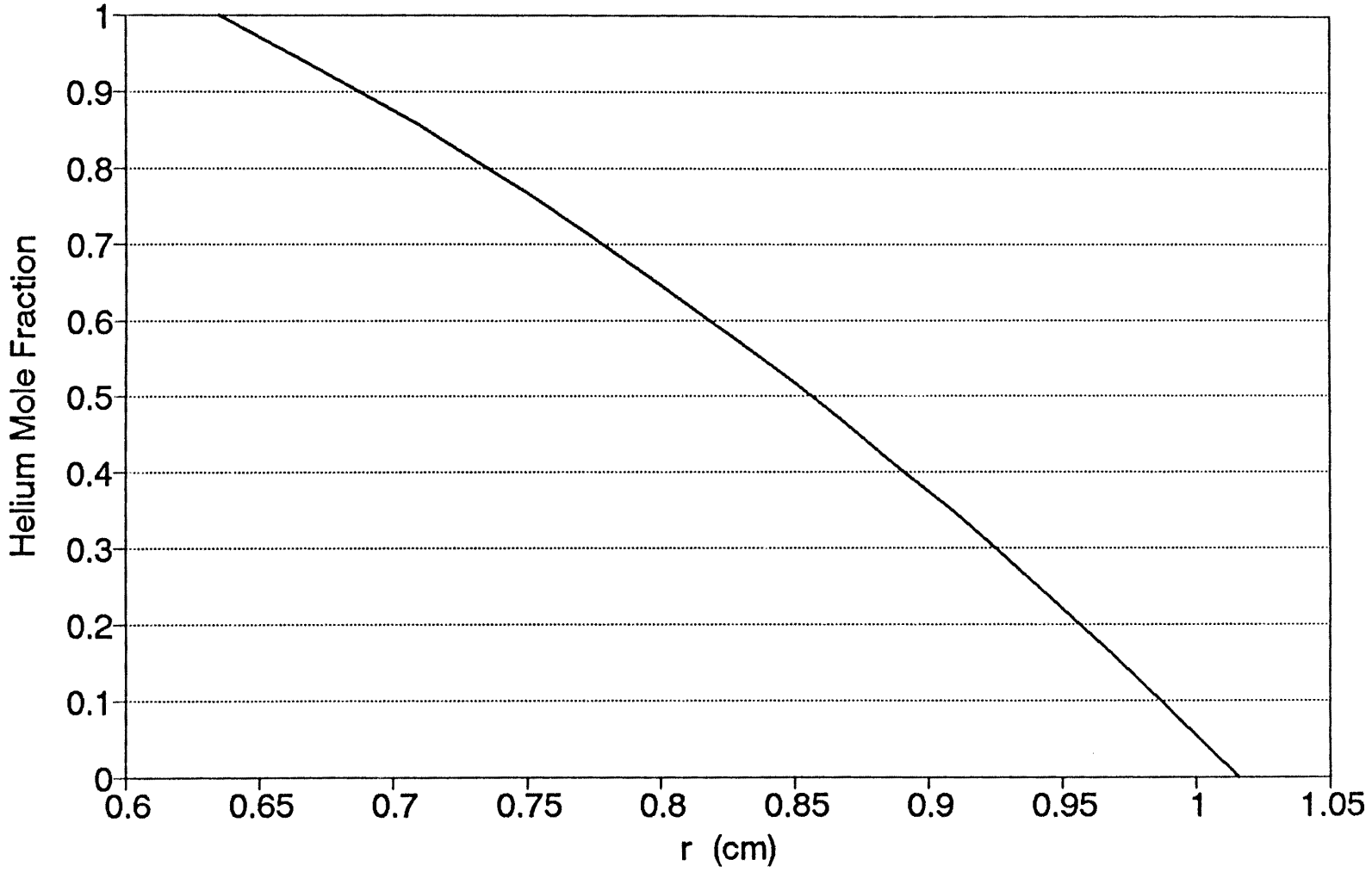

Figure 5-1. Steady radial helium distribution from Graham Model under isobaric conditions

CHAPTER 6

SUMMARY AND CONCLUSIONS

A new advective-diffusive (A-D) mathematical model for gaseous transport in porous media has been presented. The mathematical model, referred to here as the Graham Model, is applicable to gaseous transport in porous media where the molecular diffusion regime prevails, and it offers enhanced generality without added complexity when compared to existing A-D transport models. Because the Graham Model retains the traditional A-D form, the model equations readily fit into existing numerical simulators for the solution of subsurface transport problems.

The Graham Model derivation is based on the identified meaning of the Darcy advective reference velocity as a weighted average of species velocities in a gas mixture. This representation of the Darcy advective velocity is referred to here as the Graham-average velocity, and equations describing diffusive flux relative to the Graham-average velocity are derived. Neglecting pressure-, temperature-, and forced-diffusion fluxes, the Graham Model is shown to be equivalent to the Dusty-Gas Model of Mason *et al.* (1967) for cases where the molecular diffusion regime prevails. Further theoretical support for the Graham Model

is provided by showing an alternative derivation of the model using the diffusive-slip boundary condition of Kramers and Kistemaker (1943) for transport in capillary tubes, extended to porous media transport using the bundle-of-tubes analogy. It is also shown that Kramers and Kistemaker's diffusive-slip boundary condition for the mass-average velocity can be expressed alternatively as a non-slip boundary condition for the Graham-average velocity. Both molar and mass continuity equations for binary species transport are presented, along with state equations, to complete the mathematical development of the Graham Model.

For cases where gas-phase density is significantly dependent on composition, significant differences exist in the species fluxes, flux ratios, and total fluxes predicted by the Graham Model when compared to the two most common A-D transport models, the "Mole" and "Mass" Models. Of course, in cases where the phase density does not depend on composition, the Graham Model yields equivalent results to these existing, widely accepted transport models. For steady countercurrent diffusion under isobaric conditions, the species fluxes and flux ratios predicted by the Graham Model lie between the predictions of the Mass and Mole Models. Part of the difference in the model-predicted fluxes is due to differences in the diffusion equations (i.e., the different diffusion equations predict different fluxes for the same species concentration gradient), and part of the difference in model-predicted fluxes is due to

differences in the spatial distributions of species concentration predicted by each model for the same boundary conditions. Species concentration distributions predicted by the Graham Model lie between the distributions predicted by the Mole Model and the Mass Model.

The ability of the Graham Model to represent experimentally observed transport behavior has been demonstrated for a case where the gas-phase mass density is highly dependent on phase composition. The experimental data of Evans *et al.* (ET&W, 1961a) used to test the predictive capability of the Graham Model are particularly useful because the intrinsic permeability of the test medium was 2×10^{-10} cm^2. Given ET&W's test pressures, their experiments were conducted at near the lower limit of the Graham Model's applicability (where the molecular diffusion regime still prevails, but small Knudsen and Klinkenberg effects are detectable). The predictive capability of the Graham Model is compared directly to the Mole and Mass Models, which both fail to adequately represent transport processes in cases where phase mass density depends on composition. For interdiffusion cases where nonequimolar fluxes are of the same order as viscous fluxes, the total flux predictions of traditional A-D transport models can actually be of the wrong sign.

REFERENCES

Abriola, L. M., and G. F. Pinder, A multiphase approach to the modeling of porous media contamination by organic compounds, 1. Equation development, *Water Resour. Res.*, 21(1), 11-18, 1985.

Abriola, L. M., C. S. Fen, and H. W. Reeves, Numerical simulation of unsteady organic vapor transport in porous media using the dusty gas model, In *Subsurface Contamination by Immiscible Fluids, Proceedings of the IAH International Conference on Subsurface Contamination by Immiscible Fluids, Calgary, Canada*, 195-202, ed. K.U. Weyer, A.A.Balkema, Rotterdam, 1992.

Adzumi, H., Studies on the flow of gaseous mixtures through capillaries; I. The viscosity of binary gaseous mixtures, *Chem. Soc. Japan*, 12(5), 199-226, 1937a.

Adzumi, H., Studies on the flow of gaseous mixtures through capillaries; II. The molecular flow of gaseous mixtures, *Chem. Soc. Japan*, 12(5), 285-291, 1937b.

Adzumi, H., Studies on the flow of gaseous mixtures through capillaries; III. The flow of gaseous mixtures at medium pressures, *Chem. Soc. Japan*, 12(5), 292-303, 1937c.

Adzumi, H., On the flow of gases through a porous wall, *Chem. Soc. Japan*, 12(5), 304-312, 1937d.

Alzaydi, A. A., Flow of gases through porous media, Ph.D. dissertation, The Ohio State University, 1975.

Alzaydi, A. A., C. A. Moore, and I. S. Rai, Combined pressure and diffusional transition region flow of gases in porous media, *AIChE Journal*, 24(1), 35-43, 1978.

Baehr, A. L., and M. Y. Corapcioglu, A compositional multiphase model for groundwater contamination by petroleum products 2. Numerical solution, *Water Resour. Res.*, 23(1), 201-214, 1987.

Bear, J., *Dynamics of Fluids in Porous Media*, American Elsevier Publ. Company, New York, 764 pp., 1972.

Bird, R. B., Theory of diffusion, in *Advances in Chemical Engineering*, Vlo. 1, T. B. Drew and J. W. Hoopes Jr., eds., Academic Press, New York, 155-239, 1956.

Bird, R. B., W. E. Stewart, and E. N. Lightfoot, *Transport Phenomena*, John Wiley and Sons, New York, 780 pp., 1960.

Boublik, T., V. Fried, and E. Hala, *The Vapour Pressures of Pure Substances*, Elsevier Sci. Publ. Company, Amsterdam, 1973.

Carman, P. C., *Flow of Gases Through Porous Media*, Butterworths Sci. Publications, London, 182 pp., 1956.

Chapman, S., and T. G. Cowling, *The Mathematical Theory of Non-Uniform Gases*, Cambridge Univ. Press, 1939.

Clazie, R.N., G. Klein, and T. Vermeulen, Multicomponent Diffusion: Generalized Theory With Ion-Exchange Applications, Sea Water Conversion Laboratory Report No. 67-4 and Water Resources Center Desalination Report No. 19, Univ. of Calif., Berkeley, 1967*.

*Note that the above referenced report (Ron Clazie's Ph.D. Dissertation) was re-published, unaltered, by T. Vermeulen, who was listed as the sole author. The following is the reference for this second publication of Ron Clazie's Ph.D. work:

Vermeulen, T., Multicomponent Diffusion: Generalized Theory With Ion-Exchange Applications, U. S. Dept. Inter., Office of Saline Water, R&D Prog. Rep. No. 326, 1968.

Corapcioglu, M. Y., and A. L. Baehr, A compositional multi-phase model for groundwater contamination by petroleum products 1. Theoretical considerations, *Water Resour. Res.*, 23(1), 201-213, 1987.

Corey, A. T., and W. D. Kemper, Concept of total potential in water and its limitations, *Soil Sci.*, 91, 209-302, 1961.

Corey, A. T., and A. Klute, Application of the potential concept to soil water equilibrium and transport, *Soil Sci. Soc. Am. Jour.*, 49(1), 3-11, 1985.

Cunningham, R. E., and R. J. J. Williams, *Diffusion in Gases and Porous Media*, Plenum Press, New York, 275 pp., 1980.

Cussler, E. L., *Multicomponent Diffusion*, Elsevier Scientific Publishing Company, Amsterdam, 1976.

Cussler, E. L., *Diffusion: Mass Transfer in Fluid Systems*, Cambridge Univ. Press, 1984.

Darcy, H., *Les Fontaines Puliques de la Ville de Dijon*, Dalmont, Paris, 1856.

deGroot, S. R., and P. Mazur, *Non-Equilibrium Thermodynamics*, North-Holland Publ. Company, Amsterdam, 1962. (Reprinted by Dover Publ., New York, 510 pp., 1984.)

Evans, R. B. III, J. Truitt, and G. M. Watson, Interdiffusion of helium and argon in large-pore graphite, *J. Chem. Eng. Data*, 6(4), 522-525, 1961a.

Evans, R. B. III, G. M. Watson, and E. A. Mason, Gaseous diffusion in porous media at uniform pressure, *J. Chem Phys.*, 35(6), 2076-2083, 1961b.

Evans, R. B. III, G. M. Watson, and J. Truitt, Interdiffusion of gases in a low-permeability graphite at uniform pressure, *Jour. Appl. Phys.*, 33(9), 2682-2688, 1962a.

Evans, R. B. III, G. M. Watson, and E. A. Mason, Gaseous diffusion in porous media. II. Effect of pressure gradients, *J. Chem Phys.*, 36(7), 1894-1902, 1962b.

Evans, R. B. III, G. M. Watson, and J. Truitt, Interdiffusion of gases in a low-permeability graphite. II. Influence of pressure gradients, *Jour. Appl. Phys.* 34(7), 2020-2026, 1963.

Fahien, R. W., *Fundamentals of Transport Phenomena*, McGraw-Hill Book Company, New York, 580 pp., 1983.

Falta, R. W., I. Javandel, K. Pruess, and P. A. Witherspoon, Density-driven flow of gas in the unsaturated zone due to the evaporation of volatile organic compounds, *Water Resour. Res.*, 25(10), 2159-2169, 1989.

Falta, R. W., and K. Pruess, STMVOC Users Guide, Lawrence Berkeley Laboratory Rpt. LBL-30758, 129 pp., 1991.

Falta, R. W., K. Pruess, I. Javandel, and P. A. Witherspoon, Numerical modeling of steam injection for the removal of nonaqueous phase liquids from the subsurface, 1, Numerical formulation, *Water Resour. Res.*, 28(2), 433-450, 1992.

Farr, J.M. and D.B. McWhorter, Advective reference velocities and gas-phase diffusion in porous media, Presented at Fall Meeting, Abs. in *EOS Trans. Am. Geophys. Union*, 69(44), 1216, 1988.

Feng, C., and W. E. Stewart, Practical models for isothermal diffusion and flow of gases in porous solids, *Ind. Eng. Chem. Fund.*, 12(2), 143-147, 1973.

Graham, T., On the law of the diffusion of gases, Philos. Mag., 2, 175, 1833. (Reprinted in *Chemical and Physical Researches*, 44-70, Edinburgh Univ. Press, Edinburgh, 1876.)

Gunn R. D., and C J. King, Mass transport in porous materials under combined gradients of composition and pressure, *AIChE Jour.* 15(4), 507-514, 1969.

Hassanizadeh, M., and W. G. Gray, General conservation equations for multiphase systems, 1, Averaging procedure, *Adv. Water Res.*, 2, 131-144, 1979a.

Hassanizadeh, M., and W. G. Gray, General conservation equations for multiphase systems, 2, Mass, momenta, energy, and entropy equations, *Adv. Water Res.*, 2, 191-203, 1979b.

Hirschfelder, J. O., C. F. Curtiss, and R. B. Bird, *Molecular Theory of Gases and Liquids*, John Wiley & Sons, New York, 1249 pp., 1954.

Hoogschagen, J., Equal pressure diffusion in porous substances, *J. Chem. Phys.*, 21(1), 2096-2097, 1953.

Hoogschagen, J., Diffusion in porous catalysts and absorbents, *Ind. Eng. Chem.*, 47(5). 906-913, 1955.

Hubbert, M. King, The theory of ground water motion, *J. Geol.*, 48, 785-944, 1940.

Kipp, K. L. Jr., HST3D: A computer Code for Simulation of Heat and Solute Transport in Three Dimensional Ground-Water Flow Systems, U. S. Geological Survey, Wat. Res. Invest. Rep. No. 86-4095, 1987**.

**Note: Actually GHST3D, a gas-phase form of the HST3D code is referred to in the text.

Klinkenberg, L. J., The permeability of porous media to liquids and gases, in *Drilling and Production Practice*, American Petroleum Institute, New York, 200-213, 1941.

Knudsen, M., Die Gesetze der Molekularströmung und die inneren Reiburgsströmung der Gase Durch Röhren, *Annalen der Physik*, 28, 75-131, 1909.

Kramers, H. A., and J. Kistemaker, On the Slip of a Diffusing Gas Mixture Along a Wall, *Physica*, X(8), 699-713, 1943.

Jackson, R., *Transport in Porous Catalysts*, Elsevier Scientific Publishing Company, Amsterdam, 1977.

Jury, W. A., W. I. Spencer, and W. J. Farmer, Behavior Assessment Model for Trace Organics in Soil: I. Model Description, *J. Environ. Qual.*, 12(4), 558-564, 1983.

Mason, E. A., and B. Kronstadt, Graham's laws of diffusion and effusion, *J. Chem. Ed.*, 44(12), 740-750, 1967.

Mason, E. A., and R. B. Evans III, Graham's laws: Simple demonstrations of gases in motion, Part I, Theory, *J. Chem. Ed.*, 46(6), 358-364, 1969.

Mason, E. A., A. P. Malinauskas, and R. B. Evans III, Flow and Diffusion of Gases in Porous Media, *J. Chem. Phys.*, 46(8), 3199-3216, 1967.

Mason, E. A., A. P. Malinauskas, *Gas Transport in Porous Media: The Dusty-Gas Model*, Chem. Engr. Monogr., 17, Elsevier, New York, 194 pp., 1983.

Massmann, J., and D. F. Farrier, Effects of atmospheric pressures on gas transport in the vadose zone, *Water Resour. Res.*, 28(3), 777-791, 1992.

Maxwell. J. C., Illustrations of the dynamical theory of gases. Part II. On the process of diffusion of two or more kinds of moving particles among one another, *Philos. Mag.*, 20, 21, 1860. (Reprinted in *Scientific Papers*, Vol. 1, 392-409, Dover, New York, 1962.)

Maxwell, J. C., On the dynamical theory of gases, *Philos. Trans. Roy. Soc.*, 157, 49, 1867. (Reprinted in *Scientific Papers*, Vol. 2, 26-78, Dover, New York, 1962.)

Pinder, G. F., and L. M. Abriola, On the simulation of non-aqueous phase organic compounds in the subsurface, *Water Resour. Res.*, 22(9), 109S-119S, 1986.

Poiseuille, J. L. M., Mem. presentees par divers savants estrangers à l'Acad. Sci. Inst. Nat. France, 9, 433, 1846.

Pollard, W. G., and R. D. Present, *Phys. Rev.*, 73, 762, 1948.

Pollock, D. W., Simulation of Fluid Flow and Energy Transport Processes Associated With High-Level Radioactive Waste Disposal in Unsaturated Alluvium, *Water Resour. Res.*, 22(5), 765-775, 1986.

Pruess, K., TOUGH User's Guide, Earth Science Division, Lawrence Berkeley Laboratory, LBL-20700, NUREG/CR-4645, 78 pp., 1987.

Remick, R. R., and C. J. Geankoplis, Binary diffusion of gases in capillaries in the transition region between Knudsen and molecular diffusion, *Ind. Eng. Chem. Fund.*, 12(2), 214-220, 1973.

Rothfeld, L. B., Gaseous counterdiffusion in catalyst pellets, *AIChE Jour.*, 9(1), 19-24, 1963.

Satterfield, C. N., and P. J. Cadle, Gaseous diffusion and flow in commercial catalysts at pressure levels above atmospheric, *Ind. Eng. Chem. Fund.*, 7(2), 202-210, 1968.

Scott, D. S., and F. A. L. Dullien, Diffusion of ideal gases in capillaries and porous solids, *AIChE J.*, 8, 113, 1962a.

Scott, D. S., and F. A. L. Dullien, The flow of rarified gases, *AIChE J.*, 8, 293, 1962b.

Sleep B. E., and J. F. Sykes, Modeling the transport of volatile organics in variably saturated media, *Water Resour. Res.*, 25(1), 81-92, 1989.

Stefan, J., Uber das Gleichgewicht und die Bewegung, insbesondere die Diffusion von Gasgemengen, *Sitzber. Akad. Wiss. Wein. Ber.*, 63, 63, 1871.

Stefan, J., Uber die dynamische Theorie der Diffusion der Gase, *Sitzber. Akad. Wiss. Wein. Ber.*, 65, 323, 1872.

Thorstenson, D. C., and D. W. Pollock, Gas transport in unsaturated zones: multicomponent systems and the adequacy of Fick's laws, *Water Resour. Res.*, 25(3), 477-507, 1989.

Wakao, N., and J. M. Smith, Diffusion in catalyst pellets, *Chem. Eng. Sci.*, 17, 825, 1962.

Whitaker, S., Simultaneous Heat, Mass, and Momentum Transfer in Porous Media: A Theory of Drying, *Adv. Heat Trans.*, 14, 119-203, 1977.

Wicke, E., and P. Hugo, Gleitungserscheinungen bei der gasdiffusion, *Z. Phys. Chem.*, 29, 401, 1961.

LIST OF SYMBOLS

a = radius of Poiseuille tube or capillary

c_i = molar concentration of species i

c = total molar phase density = P/RT (for an ideal gas)

C_i = mean molecular speed of species i = $(8kT/\pi M_i)^{1/2}$

D_{ij} = molecular diffusion coefficient (for i in j)

D_{ij}^{*} = effective molecular diffusion coefficient (for i in j), accounting for the porosity and tortuosity = $D_{ij}\tau\theta_g$

$\mathbf{J}_i^{FR}$ = diffusion flux of i in units of "F", relative to the "R" advective reference velocity

k = Boltzmann constant

$\mathbf{k}$ = permeability tensor

$\mathbf{N}_i$ = molar flux of i relative to coordinates fixed on the porous medium

M_i = molecular mass of i

P = pressure

R = universal gas constant

T = temperature (°K)

$\mathbf{N}^D$ = total diffusive, diffusive-slip, or nonequimolar flux = $\mathbf{N}^T - \mathbf{N}^V$

$\mathbf{N}^T$ = total molar flux of the gas phase relative to fixed coordinates = $\mathbf{N}^D + \mathbf{N}^V$

$\mathbf{N}^V$ = viscous molar flux = that molar flux which dissipates momentum = Darcy molar flux

$\tilde{\mathbf{N}}$ = total molar flow rate over domain cross-section

$\tilde{\mathbf{N}}_i$ = molar flow rate of species i over the domain cross-section

E_A = molar phase transfer of A from liquid to gas

e_A = mass phase transfer of A from liquid to gas

R_A = molar rate of production of A by reactions

r_A = mass rate of production of A by reactions

$\mathbf{q}$ = Darcy volume flux

r = radial coordinate

V_i = partial molar volume of species i

V^o = molar volume of the mixture

x = cartesian coordinate

ρ_i = mass concentration of i

ρ = total mass phase density

μ = dynamic fluid viscosity

ν_i = species i drift velocity relative to fixed coordinates

ν^m = mass-average velocity

ν^N = mole-average velocity

ν^G = Graham-average velocity (defined in Chapter 3)

ν_s = Darcy seepage velocity = $\mathbf{q}/\theta_g$

ξ_{iF} = flux unit factor (defined in Chapter 3)

ξ_{iR} = reference frame weighting factor (defined in Chapter 3)

ω_i = mass fraction of i = ρ_i/ρ

χ_i = mole fraction of i = c_i/c

θ_g = gas-filled porosity

τ = tortuosity tensor

Superscripts and Subscripts

A,B = species subscripts

i,j = species subscripts and summation indices

D = total diffusive, diffusive-slip, or nonequimolar flux superscript

G = Graham-Model predicted flux and Graham-average velocity superscript

N = molar flux unit, Mole-Model predicted flux, and Mole-average velocity superscript

M = mass flux unit, Mass-Model predicted flux, and Mass-average velocity superscript

T = total molar flux superscript

V = viscous flux superscript

APPENDIX A

CONCENTRATION, VELOCITY, AND FLUX RELATIONS

[Modified from Bird *et al.*, 1960]

Concentrations in Binary Systems

$\rho = \rho_A + \rho_B$ = *mass density of solution* (g/cm^3)

$\rho_A = c_A M_A$ = *mass concentration of A* (g *of A*$/cm^3$ *of solution*)

$\omega_A = \dfrac{\rho_A}{\rho}$ = *mass fraction of A*

$c = c_A + c_B$ = *molar density of solution* (g-*moles*$/cm^3$)

$c_A = \dfrac{\rho_A}{M_A}$ = *molar concentration of A* (g-*moles of A*$/cm^3$ *of solution*)

$\chi_A = \dfrac{c_A}{c}$ = *mole fraction of A*

$M = \dfrac{\rho}{c}$ = *number-mean molecular mass of mixture*

$\chi_A + \chi_B = 1$

$\chi_A M_A + \chi_B M_B = M$

$$\chi_A = \frac{\dfrac{\omega_A}{M_A}}{\dfrac{\omega_A}{M_A} + \dfrac{\omega_B}{M_B}}$$

$$d\chi_A = \frac{d\omega_A}{M_A M_B \left(\dfrac{\omega_A}{M_A} + \dfrac{\omega_B}{M_B} \right)^2}$$

$\omega_A + \omega_B = 1$

$$\frac{\omega_A}{M_A} + \frac{\omega_B}{M_B} = \frac{1}{M}$$

$$\omega_A = \frac{\chi_A M_A}{\chi_A M_A + \chi_B M_B}$$

$$d\omega_A = \frac{M_A M_B d\chi_A}{(\chi_A M_A + \chi_B M_B)^2}$$

Velocities in Binary Systems

$\mathbf{v}_A$ = *velocity of species A relative to stationary coordinates*

$\mathbf{v}_A - \mathbf{v}^M$ = *diffusion velocity of species A relative to* $\mathbf{v}^M$

$\mathbf{v}_A - \mathbf{v}^N$ = *diffusion velocity of species A relative to* $\mathbf{v}^N$

$\mathbf{v}_A - \mathbf{v}^G$ = *diffusion velocity of species A relative to* $\mathbf{v}^G$

$\mathbf{v}^M$ = *mass average velocity* = $(1/\rho)(\rho_A \mathbf{v}_A + \rho_B \mathbf{v}_B) = \omega_A \mathbf{v}_A + \omega_B \mathbf{v}_B$

$\mathbf{v}^N$ = *molar average velocity* = $(1/c)(c_A \mathbf{v}_A + c_B \mathbf{v}_B) = \chi_A \mathbf{v}_A + \chi_B \mathbf{v}_B$

$\mathbf{v}^G$ = *Graham average velocity* = $\dfrac{\sqrt{M_A} c_A \mathbf{v}_A + \sqrt{M_B} c_B \mathbf{v}_B}{\sqrt{M_A} c_A + \sqrt{M_B} c_B}$

Mass and Molar Fluxes in Binary Systems

Quantity	With Respect to Stationary Axes	With Respect to v^M	With Respect to v^N
Velocity of species A (cm sec $^{-1}$)	v_A	$v_A - v^M$	$v_A - v^N$
Mass flux of species A (g cm^{-2}sec^{-1})	$n_A = \rho_A v_A$	$J_A^{MM} = \rho_A (v_A - v^M)$	$J_A^{MN} = \rho_A (v_A - v^N)$
Molar flux of species A (g-moles cm^{-2}sec^{-1})	$N_A = c_A v_A$	$J_A^{NM} = c_A (v_A - v^M)$	$J_A^{NN} = c_A (v_A - v^N)$
Sum of mass fluxes (g cm^{-2}sec^{-1})	$n_A + n_B = n = \rho v^M$	$J_A^{MM} + J_B^{MM} = 0$	$J_A^{MN} + J_B^{MN} = \rho (v^M - v^N)$
Sum of molar fluxes (g-moles cm^{-2}sec^{-1})	$N_A + N_B = N = c\, v^N$	$J_A^{NM} + J_B^{NM} = c\, (v^N - v^M)$	$J_A^{NN} + J_B^{NN} = 0$
Fluxes in terms of n_A and n_B	$N_A = \frac{n_A}{M_A}$	$J_A^{MM} = n_A - \omega_A (n_A + n_B)$	$J_A^{MN} = n_A - \chi_A (n_A + \frac{M_A}{M_B} n_B)$
Fluxes in terms of N_A and N_B	$n_A = N_A M_A$	$J_A^{NM} = N_A - \omega_A (N_A + \frac{M_B}{M_A} N_B)$	$J_A^{NN} = N_A - \chi_A (N_A + N_B)$
Fluxes in terms of J_A^{MM} and v^M	$n_A = J_A^{MM} + \rho_A v^M$	$J_A^{NM} = \frac{J_A^{MM}}{M_A}$	$J_A^{MN} = \frac{M}{M_B} J_A^{MM}$
Fluxes in terms of J_A^{NN} and v^N	$N_A = J_A^{NN} + c_A v^N$	$J_A^{NM} = \frac{M_B}{M} J_A^{NN}$	$J_A^{MN} = J_A^{NN} M_A$